Self-Organization of Nanoparticles

Implications for Interface Biology

Anders Lundgren

UNIVERSITY OF GOTHENBURG

AKADEMISK AVHANDLING

Akademisk avhandling för teknologie doktorsexamen i ytbiofysik, som med tillstånd från Naturvetenskapliga fakulteten kommer att offentligt försvaras fredagen den 25 maj 2012 kl. 13.00 i föreläsningssal Björn Folkow, Institutionen för kemi och molekylärbiologi, Medicinaregatan 11, Göteborg.

Göteborg 2012

ISBN: 978-91-628-8475-8

Self-Organization of Nanoparticles - Implications for Interface Biology

Doctoral thesis. Department of Chemistry and Molecular Biology, Interface Biophysics, University of Gothenburg, Box 462, SE-405 30 Göteborg, Sweden.

ISBN: 978-91-628-8475-8

First edition

All in-text graphics by Anders Lundgren if not stated otherwise.
Printed and bound in Ale by Ale Tryckteam AB 2012.

Till Sara

Abstract

Cells bind to their surroundings via proteins displayed on the cell surface. These interactions support the cells and are important for many cellular processes, e.g. cell migration during morphogenesis, wound healing and cancer metastasis. There is a yet unmet need for simple and robust *in vitro* models mirroring the complex molecular organization found in natural tissue. In this thesis, protein-sized gold nanoparticles were used to introduce morphological and biochemical nanopatterns on material surfaces via nanoparticle self-assembly. These surfaces were used to explore the effect of protein organization and other nanoscopic parameters on cell response.

In their simplest form, gold nanoparticles (in solution) are stabilized by negatively charged ions adsorbed onto their surfaces. It was shown that such nanoparticles, 10 nm in diameter, could self-organize on a dithiol modified gold surface under the influence of electrostatic double-layer forces. The distance between the adsorbed particles could be tuned by the ionic composition of the particle solution, which was described using classical DLVO-theory. A novel method to prepare surfaces with nanoparticle gradients, based on this mechanism, was introduced.

Prepared surfaces were used as templates for the assembly of nanopatterns of chemical entities and proteins, with a periodicity in the sub 100 nm regime, by site-specific grafting of different molecules to the particle surfaces. Patterns with specific cell-binding proteins and peptides as well as synthetic polymers were realized and characterized with SEM, imaging SPR, QCM-D and TOF-SIMS. Gradient patterns were also assembled with multiple ligands, e.g. RGD-peptides and heparin, allowing the investigation of synergistic cell stimuli.

Biochemical nanopatterns were evaluated in studies on human fibroblasts and endothelial cells, e.g. the cellular mobility was explored in response to different gradient stimuli. In a separate study, fimbria mediated adhesion of *E. coli* bacteria to nanoscopic adhesive domains was investigated. Surfaces decorated with gold nanoparticles were also shown to attenuate the complement protein cascade system via morphological alteration of adsorbed proteins. Altogether, concepts and methods presented in this thesis offer a route to systematically explore the interactions between biology and molecularly organized interfaces.

Populärvetenskaplig sammanfattning

Utanpå celler finns molekyler med vars hjälp cellen kan binda sig fast i andra celler eller till strukturer i sin omgivning. Så går det till när flera enskilda celler tillsammans formar komplicerade vävnader. Även vissa bakterier har specifika molekyler på sin yta, för att kunna binda sig fast till och infektera andra organismer. Att utforska hur dessa bindningar fungerar är viktigt, exempelvis för att förstå hur cancerceller sprider sig, eller för att förhindra spridningen av infektioner.

Under gynnsamma förutsättningar kan celler odlas på ytor och studeras i mikroskop. För att få verklighetsnära resultat, bör sådana ytor så långt möjligt efterlikna den mycket komplexa molekylära sammansättning och organisation som finns i naturliga vävnader. Detta kan vara svårt att åstadkomma eftersom de molekylära strukturerna är mycket små och näppeligen kan placeras ut på en yta var och en för sig. Den här avhandlingen beskriver en metod för att lösa detta problem genom att koppla samman de små molekylerna med lika små partiklar, s.k. *nano*partiklar av guld. Dessa partiklar finns vanligtvis i en vattenlösning, men fastnade spontant på de ytor som behandlats med vissa svavelinnehållande molekyler innan de doppades i partikellösningen.

Nanopartiklarna är så lätta att de inte påverkas av gravitationen, de är dock mycket känsliga för elektrisk laddning. Eftersom partiklarna har ett överskott av negativa joner på sin yta och därmed har likadan laddning, så stöts de bort från varandra. Genom att blanda små mängder salt i partikellösningen minskar denna effekt och partiklarna kan komma närmare varandra innan de stöts bort. Detta utnyttjades för att kontrollera hur långt ifrån varandra partiklarna kunde fästa på ytan - lite salt gav ett långt avstånd mellan partiklarna medan mer salt tillsattes för att få partiklarna närmre varandra på ytan.

En metod utvecklades också för att tillverka ytor med gradvis ökande mängd partiklar från den ena kanten till den andra. Genom att koppla olika signalmolekyler till partiklarna på dessa ytor kunde cellernas benägenhet att förflytta sig påverkas och studeras. I andra experiment studerades hur bakterien *E. coli*, en vanlig orsak till urinvägsinfektion, kunde binda in till mycket små fästpunkter på en yta. *E. coli* visade sig vara extra bra på detta då den är utrustad med långa smala utskott med ”klistriga” molekyler i spetsen, något som kan vara en bidragande orsak till dess sjukdomsalstrande förmåga.

List of publications

This thesis is based on the following papers, referred to in the text by their Roman numerals (I-IV):

I A. Lundgren, F. Björefors, L. Olofsson, H. Elwing.
Self-arrangement among charge-stabilized gold nanoparticles on a dithiothreitol reactivated octanedithiol monolayer.
Nano Letters (8) **2008**, 3989-3992

II M. Hulander, A. Lundgren, M. Berglin, M. Ohrlander, J. Lausmaa, H. Elwing.
Immune complement activation is attenuated by surface nano-topography.
International Journal of Nanomedicine (11) **2011**, 2653-2666

III A. Lundgren, Y. Hed, K. Öberg, A. Sellborn, H. Fink, P. Löwenhielm, J. Kelly, M. Malkoch, M. Berglin.
Self-assembled arrays of dendrimer-gold nanoparticle hybrids for functional cell studies.
Angewandte Chemie International Edition (50) **2011**, 3450-3453

IV A. Lundgren, M. Hulander, M. Hermansson, H. Elwing, O. Andersson, B. Liedberg, P. Sjöwall, M. Berglin.
Tuning molecular compartmentalization via nanoparticle self-assembly, implications for classical cell adhesion experiments.
In manuscript

Papers not included in the thesis

V J. Hedlund, A. Lundgren, B. Lundgren, H. Elwing.
A new compact electrochemical method for analyzing complex protein films adsorbed on the surface of modified interdigitated gold electrodes.
Sensors and actuators B: Chemical (142) **2009**, 494-501

VI A. Lundgren, J. Hedlund, O. Andersson, M. Brändén, A. Kunze, H. Elwing, F. Höök.
Resonance-Mode Electrochemical Impedance Measurements of Silicon Dioxide Supported Lipid Bilayer Formation and Ion Channel Mediated Charge Transport.
Analytical Chemistry (83) **2011**, 7800-7806

VII K. Öberg, J. Ropponen, M. Malkoch, A. Lundgren, M. Berglin.
Dendronized gold surfaces for cell-surface interactions.
In manuscript

Patent

En metod för att preparera en plan yta med en kontrollerad täthetsgradient av deponerade partiklar i nanostorlek. Svenskt patent nr: SE1050866-7.

Patent applications

A method of creating a biosensor based on gold nanoparticles assembled on monolayers of a dithiol (PCT/SE/2009/051060).

Probing Electrode/Solution Interfaces (US 2010/0204936 A1).

Conference contributions

13th IACIS International Conference on Surface and Colloid Science and the 83rd ACS Colloid & Surface Science Symposium, 2009, New York, United States. *"Real-Time Impedimetric Characterization of Molecular Self-Assembly Onto and Between Gold Nanoparticles Dispersed On Dithiol Modified Gold Surfaces."* Oral presentation.

Biomaterials Asia, 2009, Hong Kong, China. *"Binary Chemical Patterns With Nanometer Spatial Resolution - Investigation of Cell and Protein Response."* Poster.

Annual Biomaterials Meeting for Scandinavian Society for Biomaterials, 2010, Hafjell, Norway. *"Micro-Impedance Measurements as a Tool to gain New Insights to Biomaterial Surface Interactions beyond Measurements of Adsorbed Mass."* Poster.

Third International NanoBio Conference, 2010, Zürich, Switzerland. *"Gradients in Nanoparticle Density for Investigation of Biological Adhesion."* Oral presentation.

7th Nanoscience and Nanotechnology Conference, 2011, Istanbul, Turkey. *"Nanoparticle Gradients for Investigation of Cell-Surface Interactions."* Oral presentation.

Annual Biomaterials Meeting for Scandinavian Society for Biomaterials, 2011, Fiskebäckskil, Sweden. *"Nanoparticle Gradients for Investigation of Cell-Surface Interactions."* Poster.

Annual Biomaterials Meeting for Scandinavian Society for Biomaterials, 2012, Uppsala, Sweden. *"ECM-inspired Nanopatterns for Biomaterial Research."* *"Fimbria-Mediated Adhesion of E. Coli to Material Surfaces."* Oral presentations.

Abbreviations

AFM	Atomic Force Microscopy
APTES	3-aminopropyltriethoxysilane
BDS	Brownian dynamics simulations
CLSM	Confocal laser scanning microscopy
DLVO	Derjaguin, Landau, Verwey and Overbeek
DTT	Dithiothreitol
ECGF	Endothelial Cell Growth Factor
ECM	Extracellular Matrix
EDC	Ethyl(Dimethylaminopropyl) Carbodiimide
IC	Immune Complement
IgG	Immunoglobulin G
iSPR	imaging Surface Plasmon Resonance
LSA	Linear Superposition Approximation
LSPR	Localized Surface Plasmon Resonance
MPTMS	3-mercaptopropyltrimethoxysilane
NHDF	Normal Human Dermal Fibroblasts
NHS	N-Hydroxysuccinimide
ODT	Octanedithiol
PEG	Poly(ethylene glycol)
PEO	Poly(ethylene oxide)
PHSRN	Proline - Histidine - Serine - Arginine - Asparagine
QCM-D	Quartz Crystal Microbalance with Dissipation monitoring
RGD	Arginine - Glycine - Aspartic acid
RSA	Random Sequential Adsorption
SAM	Self-Assembled Monolayer
SERS	Surface Enhanced Raman Spectroscopy
SEM	Scanning Electron Microscopy
SPR	Surface Plasmon Resonance
TEM	Transmission Electron Microscopy
TOF-SIMS	Time Of Flight - Secondary Ion Mass Spectroscopy
XPS	X-ray Photoelectron Spectroscopy

Table of Contents

Preface

For a long time in the history of mankind, the main engineering challenge was to construct as large pyramids, cathedrals and steamships as possible. More recently, during the 20th century, focus shifted when a need for faster and better electronic devices pushed the development of micro fabrication techniques. When the first integrated circuit was assembled in 1958, few people could however imagine how large impact this development would have on society and everyday life. By continuous effort to engineer smaller and smaller structures, we have now reached the limit where the molecules of life; proteins and DNA, can be directly interfaced one by one. This thesis contributes to this new field of engineering biology by describing methods to arrange nanoparticles on surfaces and how this can be used to modulate proteins and cells. Right now, we can only guess how these opportunities will affect society for the coming hundred years.

A change of perspective is commonly a fruitful way to gain better knowledge. This work started as an industrial project devoted to sensing, but turned out to encompass a range of subjects of fundamental as well as applied character. Even though focus has shifted a few times, as well as my commitments, it has given me great opportunities to learn and explore. The work presented in this thesis is the result of four years of research, four very intensive, but exciting and joyful years. I am very glad having shared this and other experiences with valuable colleagues in the research group, whose support was absolutely necessary for this work.

First of all I want to acknowledge and extend my gratitude to my supervisors Professor Hans Elwing and Dr Mattias Berglin. You have created a truly interdisciplinary and creative research environment and I am grateful for your unlimited encouragement and great confidence in me, giving me freedom to

explore my own ways. I would also like to thank Mats Hulander heartily for his great contribution to this project, which gained considerably from our different experiences and perspectives. Furthermore, I would like to thank Emiliano Pinori and Dr Mia Dahlström. Even though you are more into “boats” than “nano”, I really appreciate your encouragement and friendly attitude. I would be glad for collaborating more with you in the future.

Running a technical project at a department of biology requires much external and internal collaboration. I gratefully acknowledge Professors Fredrik Höök, Pentti Tengvall, Malte Hermansson and Bo Liedberg for their valuable advice and help with both scientific and various practical issues. I also want to send special thanks to Fredrik Björefors for his contribution to the electrochemical analysis, Olle Andersson for helping me with SPR, Björn Lundgren for helping me with some programming, Niklas Hansson for making great substrates, Julia Hedlund for all her experimental work, Lars Faxälv for preparation and analysis of thrombocytes, Tobias Ekblad and Daniel Aili for valuable discussions. I also appreciate your great friendship.

I am also indebted to Linda Olofsson and Patrik Nordberg, who once initiated this project, to Yvonne Hed, Kim Öberg, Anders Sellborn, Helen Fink, Peter Löwenhielm, Michael Malkoch and Peter Sjövall who co-authored the articles, as well as to master students Alexander Toresson, Heissam Dernaika and Amir Saeid Mohammedi. I want to thank all research colleagues, technical and administrative staff at Lundberg lab for interesting discussions in the lunchroom as well as urgent assistance with instrumentation and issues of more bureaucratic nature.

Finally, I would like to thank my family for their support and especially Sara for your endless patience and love.

Varberg, april 2012

Anders Lundgren

1. Introduction

In the nanoscopic regime, complexity of life eventually comes down to biochemical interactions. On the cell surface there is a plethora of different functional proteins, which enable cells to communicate and organize into tissue. In higher organisms, cell receptors (integrins) form discrete attachments to multiadhesive proteins, e.g. fibronectin in the extracellular matrix (ECM).[1] These interactions do not only support the cells, but also provide a route for the cell to react to differences in its microenvironment. For example, cells may respond to small concentration differences of adhesive ligands and growth factors distributed in the matrix by migration and specialization.[2-4] These processes are especially prominent during morphogenesis and wound healing as new functional tissue forms.

The inherent sensitivity of cells to local microscale and nanoscale environments has been extensively explored to control cell adhesion and differentiation *in vitro*. This was partly driven by the wish to modify biomaterials and scaffolds for tissue engineering in such ways that cells integrate with materials rather than being rejected from them.[5] More recently, the use of engineered surfaces for cell culture was also motivated by an increased demand for functional cell lines. This encompasses for example stem cells for regenerative therapies and medical screening purposes.[6] Indeed, the introduction of topographical cues, which to some extent mimics the conditions in ECM, have proven to be efficient in modulating cell function, e.g. to control stem cell proliferation[7] or to reveal fundamental aspects of cell adhesion[8].

So far, biochemical nanopatterns have mainly been achieved using lithographic or scanning probe techniques. Even though continuously improved to reach higher resolution, these approaches suffer from some inherent limitations when it comes to the realization of very small, protein-sized structures. Most

important, using these methods, patterns are imposed top-down on substrates giving poor control of molecular organization. In contrast, in nature, highly functional structures e.g. lipid membranes, are characterized by a high degree of molecular organization. The high structural integrity is commonly a result of an ordered molecular self-assembly, governed by many weak intermolecular forces. Considering this, it is not surprising that self-assembly has evolved into a key approach for the fabrication of nanostructures[9]. Following this strategy, small building blocks such as molecules or nanoparticles can be arranged into patterns or even three-dimensional architectures with a resolution not reachable with conventional techniques, i.e. with nanometer or even sub-nanometer precision.

A nanoscopic building block that has received special attention is the gold nanoparticle. Gold nanoparticles can be synthesized in all sizes between two and one hundred nanometers. Furthermore, they can easily be tailored with molecules like DNA and proteins, making them ideal as building blocks for self-assembly.[10] In their simplest form, gold nanoparticles (in solution) are electrostatically stabilized by negatively charged ions, usually citrate, adsorbed onto their surfaces. According to the classical theory by Derjaguin, Landau, Verwey and Overbeek (DLVO),[11,12] interaction between charged colloids will depend strongly on the type and amount of ions present in the sol.

One of the main aims of this thesis, outlined in **paper I**, was to demonstrate how self-organization of gold nanoparticles on surfaces could be tuned by altering the ionic strength of the nanoparticle solution, and specifically how this could be used to control the distance between adsorbed particles (figure 1.1). In the three following papers (**II-IV**), this novel concept of nanopatterning was extended to more elaborate patterns with implications for interface biology. By specifically modifying distributed nanoparticles with functional molecules, peptides and proteins, my aim was to address cell-binding events at single protein level (figure 1.2).

The thesis is divided into two parts where the first section primarily aims at introducing subjects relating to the project. I provide several examples from the research project in order to describe the link between my results and previous work. In chapter 2, I further discuss self-assembly as a method for surface

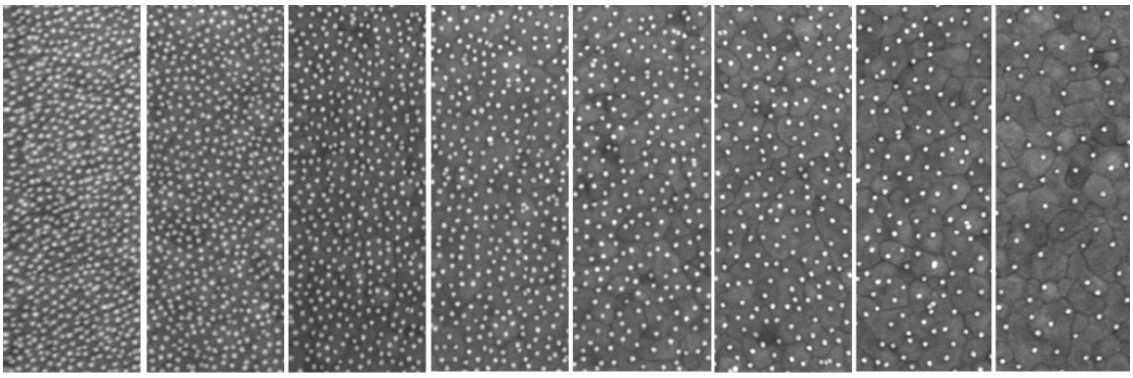

Figure 1.1 Scanning electron microscopy (SEM) micrographs from surfaces decorated with gold nanoparticles. The particles are approximately 10 nm in diameter. By altering the amount of salt in the particle solution, the distance between adsorbed particles could be tuned.

modification, the assembly of dithiols on gold substrates receiving special attention since this was a main approach for nanoparticle binding. Chapter 3 focuses on gold nanoparticles in general, whereas chapter 4 give more detailed information about the electrostatic interaction between nanoparticles in solution. Chapter 5 and 6 are devoted to nanoparticle assembly and self-organization on surfaces. In chapter 7, I give a brief introduction to cell-surface interactions, but the main focus is on site-specific chemical modifications of nanostructures. The second part of the thesis is devoted to specific results, which are presented and discussed in the four papers (**I-IV**).

To be updated. Figure 1.

Altogether, concepts and methods presented in this thesis offer a route to systematically explore the effect of nanoscopic parameters on cell response. All patterns were prepared using passive processes such as chemical self-assembly, electrostatic screening and ion-diffusion. The general concept may thus be expanded to form patterns on non-flat substrates as well as patterns with higher dimensionality. This however remains as challenges for the future.

2. Molecular self-assembly

2.1 Concepts of self-assembly

Self-assembly is often referred to as nature's own fabrication principle. This statement basis on the fact that many functional (nano) structures found in nature, e.g. cell membranes, ribosomes, and the large variety of molecular motors are spontaneously assembled as a result of weak, often cooperative, molecular interactions[1]. Indeed, the spontaneous ordering of distributed entities into predictable patterns or structures without management from an outside source is the main attribute associated with self-assembly processes.[13,14] However, an unambiguous definition of self-assembly does not exist; In this thesis I use the term "self-assembly" referring to the directed binding of molecules from solution to a surface, whereas the term "self-organization" is used to describe the assembly of nanoparticles into tunable patterns.

2.1.1 Self-assembly in the nano-workshop

Self-assembly methods for nanofabrication are still in their infancy. Compared to the intricate and highly functional structures found in nature, man-made structures prepared from synthetic building blocks appear simple. Still, inspiration from nature offer great opportunities to refine and develop new self-assembly approaches with higher complexity. For example, DNA can be arranged into advanced secondary structures, often referred to as "DNA-origami", based on the specific base pairing encoded in the primary sequence.[15] The complementarity of DNA has also been extensively used to control the assembly of other DNA-tailored building blocks, e.g. gold nanoparticles.[16,17] Similar controlled assembly of gold nanoparticles was also obtained by tailoring nanoparticles with *de novo* designed polypeptides. By adding zinc ions, peptides with random orientation on different particles folded into a predestinated secondary structure, thereby inducing particle aggregation.[18]

Another example of three-dimensional self-assembly that received much attention was nanofibers assembled from amphiphilic molecules consisting of a hydrocarbon tail and a peptide head.[19] By change of pH or ionic strength altering the electrostatic repulsion between charged peptides, these molecules could self-assemble into fibers with a hydrophobic core and peptide-decorated surface.[20] Assembly could also be achieved *in vivo* after injection, making such fibers promising candidates for regenerative biomaterials.[21]

2.1.2 Self-assembled monolayers

Compared to the three-dimensional structures, the use of self-assembly for surface modifications is well established. So-called self-assembled monolayers (SAM) are ordered assemblies of molecules formed on solid surfaces. For example, organofunctional alkoxysilane molecules can form SAMs on oxide surfaces, e.g. glass, silicon dioxide and aluminum oxide. The basis for this assembly is the formation of covalent bonds between the silane molecules and hydroxyls on the oxide surface.[22] Silanization is thus facilitated by oxidizing pre-treatments of the substrates. Silanes can be conjugated to functional groups, e.g. amine, thiol or polyethylene glycol (PEG), offering a possibility to introduce specific functionality on a surface. A drawback however, is that the preparation of silane SAMs is sensitive to many different parameters, e.g. the amount of water present during the assembly, which makes it difficult to produce SAMs with sufficient quality and reproducibility. [23]

Another SAM that can be applied on oxide surfaces, especially silicon dioxide and glass, is the supported lipid bilayer.[24] The assembly of a lipid bilayer (from spontaneous rupture of lipid vesicles) is not governed by covalent bonds, but is dependent on many cooperative weak interactions, e.g. the lateral Van-der-Waals interactions within the hydrocarbon core of the bilayer. The assembly may also be facilitated by electrostatic interactions between lipid head groups and the surface charges or by the coordination of divalent cations.[25] Use of supported lipid bilayers has increased lately since they can support membrane-embedded proteins, which may lose their activity outside the lipid environment, e.g. trans-membrane ion-channels. An example of this can be found in **paper VI** (not included in the thesis).

Yet another type of surface modification extensively used in fundamental and applied surface science is SAMs of alkanethiols on gold.[22] This type of modification is central for the work presented in this thesis, and will therefore be discussed in detail in the following sections.

2.2 Surface functionalization of gold

Self-assembled monolayers on gold were introduced by Nuzzo and Allara in 1983, when they described the functionalization of gold surfaces by adsorption of disulfides.[26] Since then, among the organosulfuric compounds, predominately thiols have been used for formation of SAMs on gold. Especially the behavior of SAMs assembled from different alkanethiols was extensively investigated by Whitesides[27], Ulman[22] and Porter[28], to mention a few.

2.2.1 Self-assembled monolayers of alkanethiols

The use of alkanethiol SAMs has become a standard approach for construction of model surfaces used for gaining a deeper understanding of interfacial phenomena, e.g. protein adsorption[27,29,30]. This can easily be understood considering their versatility; without affecting the mechanisms of monolayer formation, SAMs from alkanethiols can be constructed displaying almost any chemical functionality to the surrounding environment.[27] Alkanethiol SAMs are also extensively used within biosensor applications, especially for SPR (Surface Plasmon Resonance)[31] or electrochemical approaches where gold is commonly used on sensors and electrodes[32,33].

The assembly of alkanethiols onto gold surfaces is a two-step process, starting with the very rapid adsorption of thiols to all available binding sites on the surface. This process is governed by the formation of strong, covalent thiolate-bonds to the gold surface (binding strength ~170 kJ/mol)[34]. The initial adsorption is followed by a much slower (several hours) reorganization and structuring of the adsorbed thiols[27].

This process is driven by weak lateral interactions between, primarily, the hydrocarbon parts of the molecules. As a result, the thiols form a hexagonal

(√3X√3)R30° adlayer on the Au(111) lattice (Figure 2.1), where the alkyl chains order themselves in a slightly tilted, all trans configuration that allows optimal lateral interaction between the molecules.[22] However, the exact conformation depends on the length of the alkyl chains. For chains with less than 12 carbon atoms, the SAM exhibits an increasing degree of unordered structure at the top of the monolayer (all trans-gauche) and for chains with less than eight carbon atoms, the structure is totally unordered (gauche)[35].

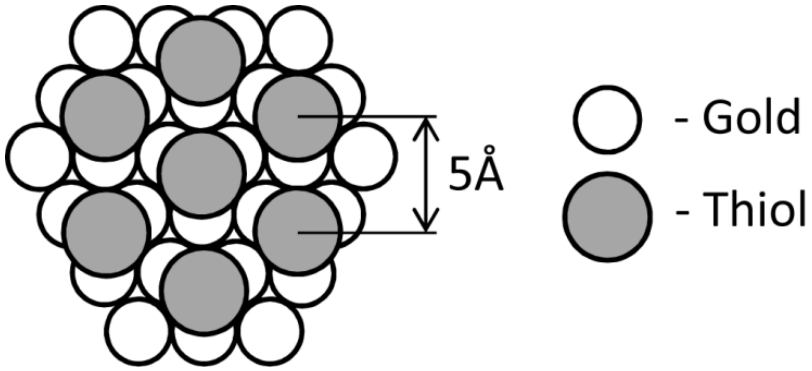

Figur 2.1 On the Au(111) crystal lattice, alkanethiols form a hexagonal (√3X√3)R30° adlayer with approximately 5Å between neighboring sulfur atoms.

The procedure for preparation of thiol SAMs is straightforward, even though special caution is necessary considering cleanliness in order to avoid contamination of the gold surfaces. The gold substrates are, subsequent to extensive cleaning, immersed in thiol solution. Normally ultra-pure ethanol is an appropriate solvent for thiols having up to 18 methylene units. For longer thiols an organic solvent, e.g. hexane has to be used. Besides the solvent, also the temperature, immersion time and quality of the gold substrate are important parameters determining the quality of the SAM.[27,35]

2.2.2 Self-assembled monolayers from smaller thiols

Since the degree of order within the monolayer structure decreases with decreasing chain length, monolayers made from smaller thiols are not well structured and may therefore form SAMs with lower molecular density than long-chain alkanethiols.[36] However, if the molecular organization is not considered the most important feature, but rather the surface functionality, using such SAMs might be a good idea. Commonly used thiols are, among others,

mercaptopropionic acid (negatively charged), cysteamine (positively charged) and cysteine (zwitterionic). Cysteine is of special interest since it has been shown that cysteine form monolayers on gold with both the amino groups and the carboxyl groups freely protruding away from the surface.[37] This is interesting since both amine and carboxyl groups constitute good handles for covalent coupling of for example proteins.[38]

The smallest thiols can often be deposited from aqueous solvents and buffered solutions. This is advantageous for the surface functionalization of gold nanoparticles in solution, as will be further discussed in the following chapters. The high solvability and low degree of organization also make it easy to remove smaller thiols from the surfaces. In **paper II** it was shown that cysteamine, used to promote adsorption of nanoparticles, could be completely removed from the surface after particle deposition by immersion in an oxidizing bath.

2.3 Self-assembled monolayers for nanoparticle binding

Self-assembled monolayers have been extensively used to immobilize nanoparticles, especially gold nanoparticles, to surfaces. The objects were mainly bottom-up fabrication of nanodevices, development of biosensor applications and preparation of substrates for surface enhanced Raman spectroscopy (SERS).[10,39]

A majority of the methods involve self-assembly of citrate stabilized gold nanoparticles to a SAM. For glass and other silicon-based substrates, especially SAMs of (3-mercaptopropyl)-trimethoxysilane and (3-aminopropyl)-triethoxysilane have been utilized.[40] These SAMs display thiol respectively amino groups, which can capture gold nanoparticles from solution. For gold substrates, the dominating method for gold nanoparticle assembly is the use of the thiol cysteamine (aminoethanethiol), which forms monolayers displaying amino groups. Compared to amine functional SAMs, more persistent binding of gold nanoparticles can be obtained with SAMs of dithiols, i.e. homobifunctional thiols that optimally assemble on gold with one free sulfhydryl.

2.3.1 Dithiol monolayers with enhanced reactivity

Dithiols have been widely used to attach gold nanoparticles to surfaces and structures, however dithiol molecules are prone to form poorly organized multilayers and the modified surfaces often display uneven and irreproducible nanoparticle binding compared to amine functional surfaces. The issue of molecular orientation within dithiol layers is still up for discussion. Structural investigations indicate both that molecules can adopt a flat configuration on the surface as well as upright aligned configurations depending on the sample preparation [41,42] It has been pointed out that the lack of control of oxidants may be responsible for the variable reactivity observed for dithiols. Samples prepared in the presence of oxygen exhibited different degrees of adsorbed disulfide structures. The formation of loop structures, i.e. dithiolates on the surface has however been ruled out by most studies [43,44]

An important finding in our laboratory was that the reactivity of a self-assembled monolayer of a linear standard alkanedithiol (1,8-octanedithiol, herein abbreviated ODT) prepared from ethanolic solution could be significantly enhanced by reactivation of an ODT SAM with dithiothreitol (DTT). DTT, also referred to as Cleland's reagent[45], is a common reagent for reduction of inter- or intramolecular disulfide bonds in proteins and is used in many biochemical methods. We noted that after treatment with DTT, the homogeneity of an adsorbed layer of citrate stabilized gold nanoparticle was significantly enhanced and that this procedure gave very reproducible results. The reproducibility was further increased by repeated incubations in first ODT and then DTT just before nanoparticle assembly. A detailed protocol for the preparation of DTT reactivated ODT monolayers can be found in **paper I**.

A hypothetical mechanism for the enhanced reactivity of the dithiol SAM is that DTT reduces intermolecular disulfides within the SAM. (Figure 2.2) This way dithiols can align better and display more surface thiolates. In the initial stage, there might also be an excess of dithiols on the surface, not bound to the gold but polymerized to each other. This could be the reason for the numerous observed areas (<100 nm) without any bound particles. During DTT treatment polymerized dithiols are removed, leaving a true orthogonally arranged monolayer.

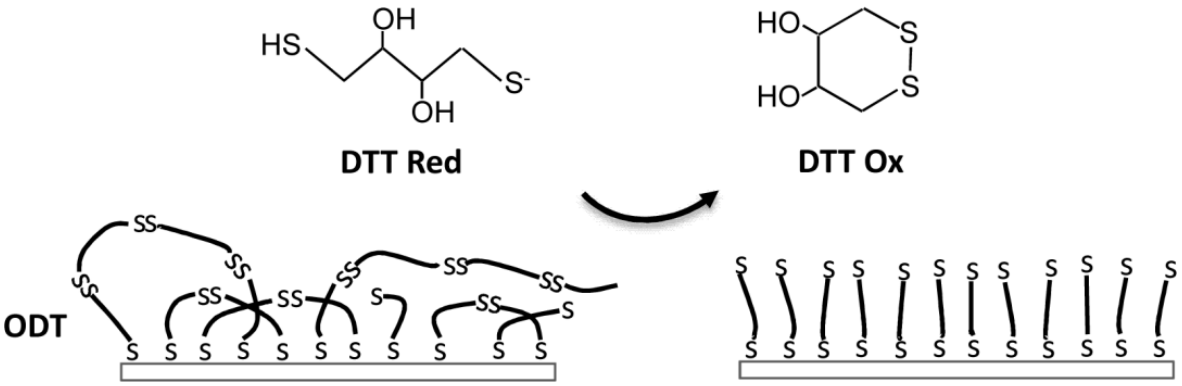

Figure 2.2 Hypothetical mechanism for the enhanced reactivity of ODT-modified gold observed after treatment with DTT. Intermolecular disulfides are reduced via DTT mediated thiol-disulfide exchange reactions

2.3.2 Voltammetric evidence for monolayer restructuring

To support the hypothesis that reaction with DTT can improve the surface organization of pre-assembled ODT, ellipsometry[46] was performed to measure any change in layer thickness due to the DTT treatment. Cyclic voltammetry[47] was also employed to measure the charge transfer associated with reductive desorption of bound dithiols from the gold surface. By integrating the charge under the reductive peaks, the thiol surface coverage can be determined.[48] Furthermore, the peak positions in the cyclic voltammogram also reflect the molecular interaction within the layer, e.g. molecular packaging.[49-52] A detailed description of the instrumentation and procedures can be found in the supporting information of **paper I**. The reductive desorption of the ODT monolayers was examined before and after reaction with DTT. Also the reductive desorption of DTT alone and after two repeated incubation cycles with ODT and DTT was examined. Cyclic voltammograms are presented in figure 2.3 and summarized in table 2.1.

After treatment with DTT the thickness of the ODT layer increased from about 10 Å to about 13 Å, corresponding well to the molecular length of a fully extended ODT molecule.[53,54] The thickness of a DTT monolayer was in comparison only about 7 Å, indicating that the DTT was not capable of substituting the ODT during the DTT treatment.

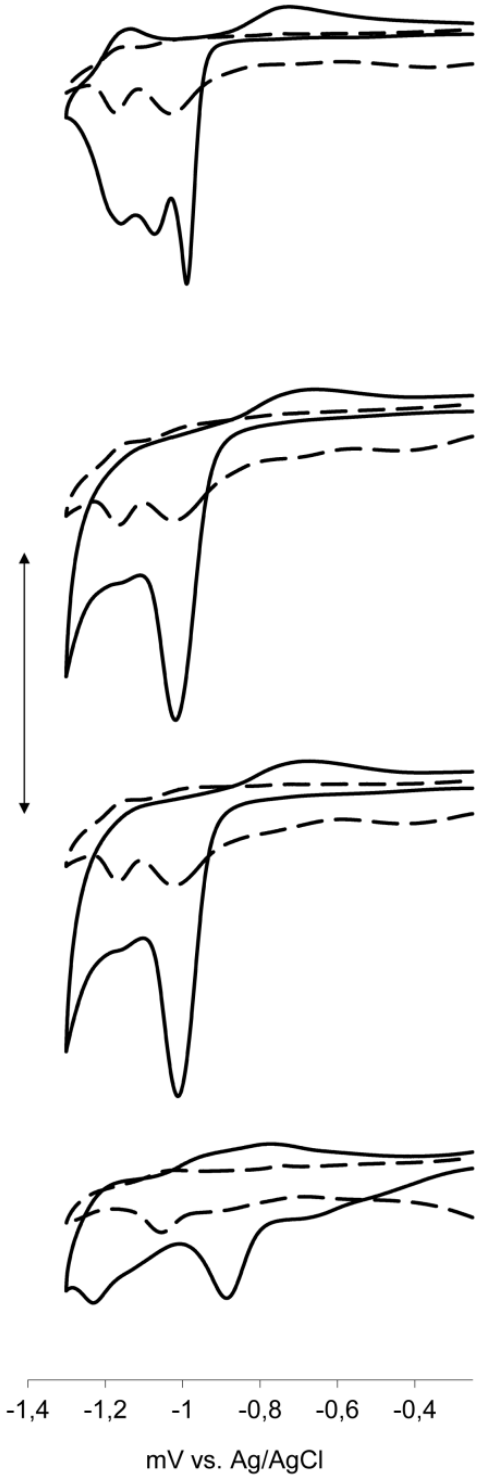

Figure 2.3 The reductive desorption of ODT on gold surfaces was examined before and after treatment with DTT. The reductive desorption after two sequential treatments with ODT and DTT as well as treatment with DTT alone was also examined. Measurements were done in 0.1M KOH at 200mV/s scan rate. Thick lines are the first reductive and oxidative scan, broken lines are the second reductive and oxidative scan. The scalebar is 50 μA.

Table 2.1

Ellipsometric thickness[a]

	ODT (Å)	ODT +DTT (Å)	ODT +DTT Repeated (Å)	DTT (Å)
Thickness[a]	10.2 ±0.3	-	12.8 ±0.4	6.7 ±0.4

First reductive and oxidative scan[b]

	ODT (mV vs. Ag/AgCl / μC/cm$^{2)}$)	ODT +DTT (mV vs. Ag/AgCl / μC/cm$^{2)}$)	ODT +DTT Repeated (mV vs. Ag/AgCl / μC/cm$^{2)}$)	DTT (mV vs. Ag/AgCl / μC/cm$^{2)}$)
1:st reductive peak	-996±16 / 152±8[c]	-1023±10 / 93±11	-1015±6 / 95±6	-880±2 / 23±2 -662±2
2:nd reductive peak	-1076±11 / 152±8[c]	- / -[d]	- / -[d]	- / -[d]
3:rd reductive peak	-1159±4 / 152±8[c]	-1158±3 / -[d]	-1156±1 / -[d]	-1227±1 / 14±17 -1113±27
1:st oxidative peak	-1151±0 / 10±1	- / -[d]	- / -[d]	-1200±2 / 5±2
2:nd oxidative peak	-734±4 / 20±0	-698±6 / 19±2	-698±7 / 21±2	-777±10 / 30±7 -967±9

Second reductive and oxidative scan[b]

	ODT (mV vs. Ag/AgCl / μC/cm$^{2)}$)	ODT +DTT (mV vs. Ag/AgCl / μC/cm$^{2)}$)	ODT +DTT Repeated (mV vs. Ag/AgCl / μC/cm$^{2)}$)	DTT (mV vs. Ag/AgCl / μC/cm$^{2)}$)
1:st reductive peak	-1025±3 / 19±1	-1018±3 / 18±1	-1017±2 / 19±2	-1046±9 / 26±12 -897±5
2:nd reductive peak	- / -[d]	- / -[d]	- / -[d]	- / -[d]
3:rd reductive peak	-1170±2 / 8±1	-1165±3 / 7±0	-1165±1 / 7±0	- / -[d]
1:st oxidative peak	-1165±3 / 2±0	-1159±4 / 2±1	-1157±1 / 2±0	- / -[d]
2:nd oxidative peak	-1002±4 / 2±1	-988±7 / 2±0	-986±9 / 3±1	-1029±9 / 4±1 -744±3

[a] The presented value is the mean of at least three surfaces with five measurements on each surface. The standard deviation is the pooled standard deviation from the measurements on each surface. [b] Values for peak position and charge is the mean and standard deviation of at least three surfaces. [c] Charge represent the total integrated charge for all peaks 1, 2 and 3 since the peaks overlap too much to be measured individually.
[d] Refers to no peak, or that the peak is too small to determine its exact location and/or area.

Reductive desorption of the differently treated ODT layers showed that treatment with DTT reduced the number of reductive peaks during the first reductive scan, whereas no difference was observed during the second scan. It is well established that regions of different[50] or differently organized[49,51,52] thiols on a gold electrode may give rise to more peaks in the reductive voltammogram. Thus, this result indicates that the ODT layer had a heterogeneous structure before the DTT treatment and became more homogenous after the treatment.

After reduction with DTT, the integrated charge for the ODT desorption (after subtraction of the capacitive contribution) was 95±6 μC/cm^2. This is close to or slightly above the usually accepted value 85±10% μC/cm^2 corresponding to a full (mono)thiol monolayer.[52] The integrated charge for the ODT layer without DTT treatment is much higher, which indicates the presence of disulfide-bounds within the molecular layer. Cyclic voltammetry on surfaces treated with only DTT showed no interfering peaks with the DTT treated ODT layers. Altogether, the results from ellipsometry and voltammetric desorption measurements strongly indicate that the surfaces treated with octanedithiol and subsequently dithiothreitol acquire well-organized octanedithiol monolayers rather than an exchange of octanedithiol for dithiothreitol.

The high homogeneity of the dithiol SAMs that were obtained after DTT-reactivation, allowed dithiol modified gold surfaces to be used for nanoparticle assembly. A uniform surface coverage with few defects was achieved also on relatively large surfaces. Since the influence of defects on the organization of nanoparticles was minimized, rational investigation of other parameters influencing the particle organization became straightforward. This modification strategy was therefore used to explore the electrostatic self-arrangement of nanoparticles in **paper I**. The homogenously distributed dithiols could also be used as a chemical handles to which other molecules could be grafted. This was employed in **paper III** and **IV** for the fabrication of chemical nanopatterns.

3. Gold nanoparticles

In the age of nanotechnology, research related to gold nanoparticles is of current interest. Nevertheless, colloidal gold is in fact a very old invention. The first time "soluble gold" appears is probably in Egypt and China around the 5th or 4th century B.C. Back then, colloidal gold was primarily appreciated for esthetic reasons. The solutions, which could contain a spectrum of colors from yellowish pink and deep ruby red to dark violet, were used for coloring of glass and ceramics. Historically, gold solutions also had a reputation of possessing powerful curative properties and were used as a general remedy for almost any disease.[10]

During the 18th century, it was established that the soluble gold actually consisted of gold particles in solution. A French dictionary from 1769 stated; "Drinkable gold contained gold in its elementary form but under extreme sub-division suspended in a liquid". Examinations of the colloidal gold were continued during the 19th century when Faraday reported a famous way to prepare gold colloids through reduction of chloroaurate ($AuCl_4^-$) using white phosphor.[55] Faraday also investigated the optical properties of the gold colloids and his work was coming to be important for the emergent field of colloidal science.

During the 20th century, different methods for preparation of gold colloids were presented and reviewed.[56-59] The last decades have meant a renaissance for the gold colloids. This time it had nothing to do with the colloid solutions' bright and beautiful colors in the context of art and craftsmanship, but rather with the colloids' optical and electronic properties at single particle level. During the 1980's and 1990's gold colloids gained interest within the field of cytochemistry.[60] Gold colloids bound to various antibodies, lectines and other proteins used for immunocytochemistry gave accurate signals in the transmission and scanning electron microscopy. This led to refined protocols for preparation and size separation of gold colloids.[61]

A large number of publications involving gold colloids have been published recently, in the context of nanotechnology, sensing and self-assembled monolayers. Here, the gold colloids are often referred to as gold nanoparticles.[10,62] The popularity of gold nanoparticles is partly based on quantum size effects giving rise to electronic[33,54,63] and optical behavior[64] that can be utilized for different sensing applications.[65-67] Another important factor is that gold nanoparticles are quite stable and that they can be fabricated with sizes between 1 and 100 nm, making them excellent building blocks for applications below the limit for standard lithographic techniques but larger than the molecular level.[62]

3.1 Synthesis of gold nanoparticles

As implied, it has been known for quite some time how to synthesize gold colloids, and many different technical approaches exist. Recently two main routes for synthesis of nanoparticles especially well-suited for the construction of devices and nanostructures have become standard.

3.1.1 Turkevich method

The by far most popular method used for gold nanoparticle synthesis is reduction of gold salt, commonly $AuCl_4^-$ with citrate as reducing agent in aqueous solution. This very simple method, introduced by Turkevich in the 1950's, yields roughly spherical particles smaller than 100 nm in diameter.[56] The size is controlled by the initial citrate to $AuCl_4^-$ ratio, where higher ratios give smaller particles.

For the preparation of the smallest particles (<10 nm) the use of an additional reductive agent, e.g. tannic acid is optimal.[61] The tannic acid will cause a fast nucleation where the number of nuclei is determined by the amount of tannic acid. Since the synthesis is limited by available gold ions, the number of nuclei will effectively determine the particle size. The gold nanoparticles used in the thesis works were prepared using an extension of the tannic acid/citrate reduction method. Protocols were developed to produce any particle size in the range 5-30 nm (figure 3.1) with narrow size distribution (±10%).

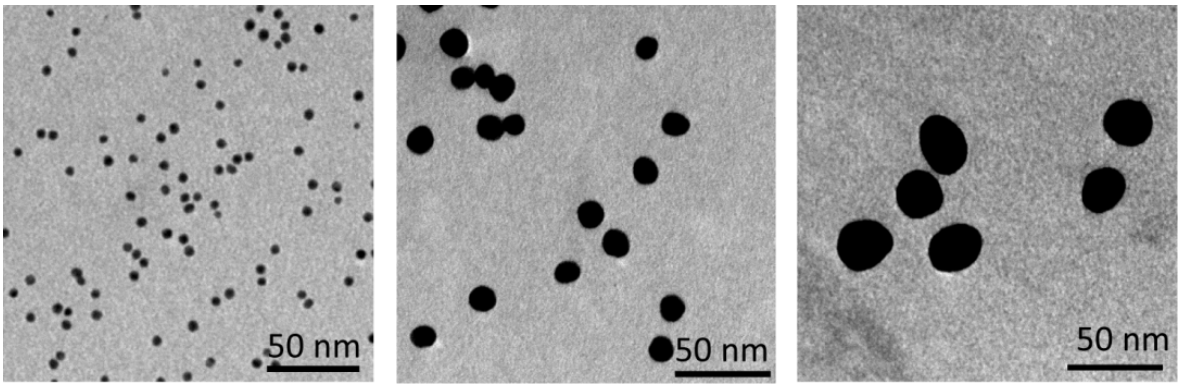

Figure 3.1 TEM micrographs of gold nanoparticles, 5 nm, 15 nm and 25 nm, used in the project. Photo courtesy of Dr Jenny Lindström.

During synthesis, citrate ions adhere loosely to the gold core, providing the particle surfaces with a negative net charge that stabilizes the particle in solution. The stability is however susceptible to the binding of organic molecules, pH, and addition of salts as will be further discussed in the following sections. Since the particles are obtained in water, these particles are suitable for applications involving biomolecules.

3.1.2 Brust-Schiffrin method

The second commonly used method for gold nanoparticle synthesis was established as late as 1994 by Brust et al.[58] In this method, the reduction of $AuCl_4^-$ is not performed in aqueous solution, but the salt is transferred to an organic solvent using a transfer agent. In the organic solvent, the gold ions are reduced by addition of a reducing agent, commonly $NaBH_4$. In the presence of long-chain alkane thiols, which bind to the nanoparticle surface, the nanoparticles are stabilized due to steric interaction between alkane chains of different particles.

In contrast to the Turkevich method, this protocol yields particles that are thermally and air stable, and easily can be transferred between different organic solvents. By altering the thiol to $AuCl_4^-$ ratio in the preparation, particles with narrow size distributions having mean core diameters ranging between 1.5 and 5.2 nm can be produced.[68] The core size decreases with increasing thiol to gold ratio. Alkanethiol stabilized particles have gained attention since they constitute a particle analogue to the flat substrate SAMs. As the conventional SAMs these

particles have shown promising results regarding the possibility to provide surface functionality, multiple functionalities etc. to the particles.[69]

3.2 Optical properties

In contrast to the well-known yellowish color of bulk gold, the nanoparticles display a deep-red color. By addition of salt or change of pH, the color of the solution may change through a spectrum of colors to different degrees of violet, blue and black (figure 3.2).

The phenomenon was described in detail by Mie who developed a solution of Maxwell's equations for the interaction between electromagnetic fields and small spheres.[70] In accordance with Mie theory, the bright colors are attributed to dipole oscillations of the free electrons confined in the conduction band of the metallic sphere. If this oscillation couples with an incoming electric field, resonance occurs and energy corresponding to the resonance frequency is adsorbed (figure 3.2). The phenomenon is referred to as nanoparticle plasmon resonance or localized surface plasmon resonance (LSPR) in order to distinguish the phenomenon from surface plasmon resonance (SPR), which arises at flat interfaces.

3.2.1 Influence on LSPR due to particle size

A main characteristic for the LSPR of gold nanoparticles in the size-range between 1 and 40 nm, is the peak extension in the visible spectra around 520-530 nm. Experimental results indicate that the exact position and magnitude of the extinction peak are influenced by the particle size. For examples, particles with a mean diameter of 9, 15, 22, 48 and 99 nm showed maximum extinction at 517, 520, 521, 533 and 575 nm, respectively. The sharpest peak could be seen for particles with an average size of 22 nm, whereas smaller and larger particles gave broader peaks.[71]

For particles smaller than 2 nm, the LSPR diminishes completely as the energy levels for the electrons become discrete and instead step-like spectral transitions occur.[10]

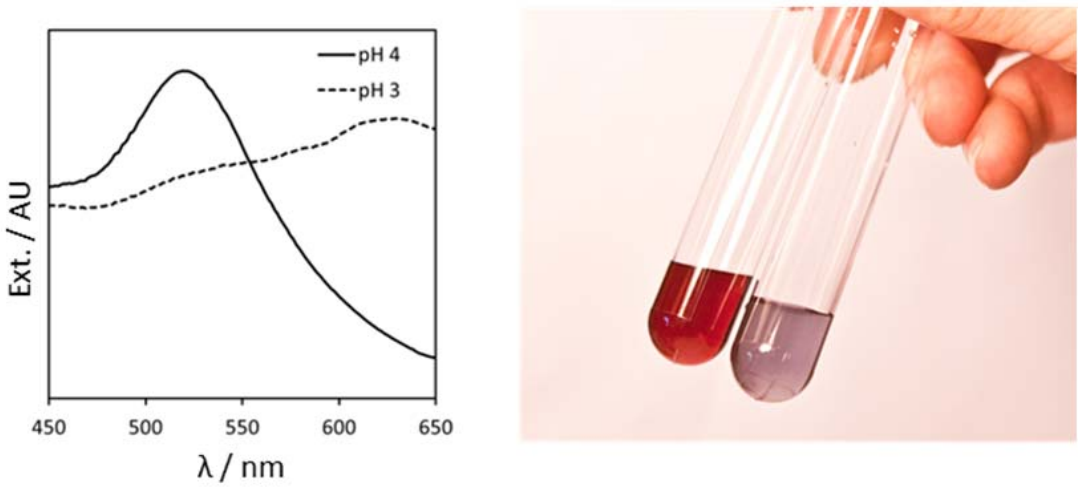

Figure 3.2 The localized surface plasmon resonance gives gold nanoparticles a deep red color characterized by an extinction peak in the visible spectra. The color change when particles aggregate, e.g. by changing pH of the particle solution.

3.2.2 Influence on LSPR due to surrounding media

The LSPR will also be affected by the refractive index of the ambient medium since the polarization of the particles will induce an opposing polarization in the ambient media. It has been shown that for a series of liquids not interacting chemically with the surface, but with increasing refractive indexes from 1.33 for water to 1.50 for toluene, a stepwise shift of the LSPR peak to longer wavelengths was observed. The magnitude of this shift in wavelength was however not large, only about 10 nm.[67,72] Even though these shifts can be predicted qualitatively using Mie theory, the exact values obtained from theoretical calculations seldom agree with experimental results. The reason is that ordinary Mie theory deals with naked nanoparticles, whereas in reality a ligand shell that stabilizes the solution always surrounds the particles.[10]

In order to make predictions that correlate with the experimental results, models have to be created where the Mie theory is adopted to include contributions from stabilizing and/or functionalizing ligands close to the nanoparticles. Such models can also be used to evaluate the behavior of biosensors where functional ligands are conjugated to gold nanoparticles.[73] Even though the shift obtained in the LSPR spectra upon a change of refractive index is relatively small, the measurement is straightforward and many biosensors based on this mechanism have been proposed. In most cases, gold nanoparticles were then immobilized to a transparent or reflecting surface, whereupon the transmission/reflection extinction spectra from the particles could be obtained.[67]

3.2.3 Influence on LSPR due to particle separation

For two or more nanoparticles in contact, the resonance frequency will shift relative to that of the single uncoupled resonator due to near-field coupling.[74] In the LSPR spectra, this can be seen as a shift of the resonance peak to longer wavelengths, i.e. a red shift as well as peak broadening. Compared to the shifts induced by changes in the refractive index of ambient media, the shifts caused by inter-particle coupling are very large. The dramatic and fascinating color changes seen in gold nanoparticle solution can thus mainly be attributed to aggregation of the particles in solution.

The magnitude of the red shift due to aggregation is controlled by several factors where the most important are aggregate size, the interparticle distance and the particle size.[10,62,74] The more particles being in contact, the longer the range of the plasmon coupling and the shift of the LSPR peak. The absolute distance between the particles in the aggregate (the ratio between inter-particle distance and particle), also influences the magnitude of the shift. It has been shown, by theory and experiment, that with increasing particle spacing the LSPR shift decay exponentially until the distance exceeds about twice the particle diameter. For longer distances, the plasmon-plasmon coupling effects can be neglected.[74] This means that for particles linked by protein or other biomolecules, the shift observed is smaller than for particles aggregated by addition of salt.

For practical work with gold nanoparticles, analyzing the color of the particle solution is an efficient way to ensure the state of the particles, e.g. to ensure that particles are not aggregated before use. The color shifts induced by aggregation has also been extensively used to detect the specific assembly or disassembly of bio-functionalized nanoparticles in biosensor applications.

4. Colloidal stability & DLVO-theory

In solution, nanoparticles are subject to temperature dependent Brownian motion. If the particle concentration is high, particles will frequently collide, eventually leading to irreversible aggregation and precipitation. To keep particles dispersed in solution, particle surfaces must therefore be provided with some stabilizing agent that induces repulsion between adjacent particles. Two mechanisms are commonly used to achieve stable particle solutions: steric stabilization or electrostatic stabilization.

4.1 Steric and electrostatic stabilization

Nanoparticles can be straightforwardly stabilized by adsorption of large, bulky molecules, e.g. polymers, onto their surfaces. As the modified particles approach each other, the surface-bound molecules must reorganize or compress due to the size exclusion effect. Thereby, the conformational entropy of the individual molecules decreases, resulting in a net repulsive force between the particles. If the compression also imposes rearrangement of water molecules associated to the particle surfaces, additional hydration forces may arise.[75] Since the origin of the repulsive force is due to steric restrictions, this technique to stabilize particles is often referred to as *steric stabilization*. Such particles often display very high stability towards the effects of drying, salt, changes in pH etc. and are therefore suitable for large-scale processes outside the controlled laboratory environment. For example, particles prepared according to the Brust-Schiffrin method are sterically stabilized by the alkanethiol SAM they receive during synthesis.

In the case of citrate-mediated particle synthesis, the citrate does not only work as reductive agent, but it also provides particle stabilization.[76] During reaction, excess citrate adheres to the gold core forming a shell of negatively charged ions around the particle. The citrate layer is too thin and too loosely bound to withstand compression, however the negative net charge may stabilize the

particles due to electrostatic interactions across the aqueous media. This type of stabilization is referred to as *electrostatic stabilization* or *charge stabilization*, and is best described within the framework of DLVO-theory.

4.2 DLVO-theory

The DLVO-theory is probably the most important theoretical work within colloid and interface science. Rather than a single theory, it is a framework based on the works presented by Derjaguin and Landau in 1941[12] and Verwey and Overbeek in 1948.[11] Within the DLVO-framework, all interactions between colloids and surfaces with electrostatic origin are treated and described in terms of distance-dependent interaction potentials, i.e. *U(D)* where *U* is the free energy and *D* is the surface separation. As indicated in figure 4.1, the interaction potential consists of attractive Van der Waals interactions and repulsive double-layer interactions. The sum of attractive and repulsive interactions gives the characteristic total potential profile with a peak in the repulsive regime at a few nanometers of separation.

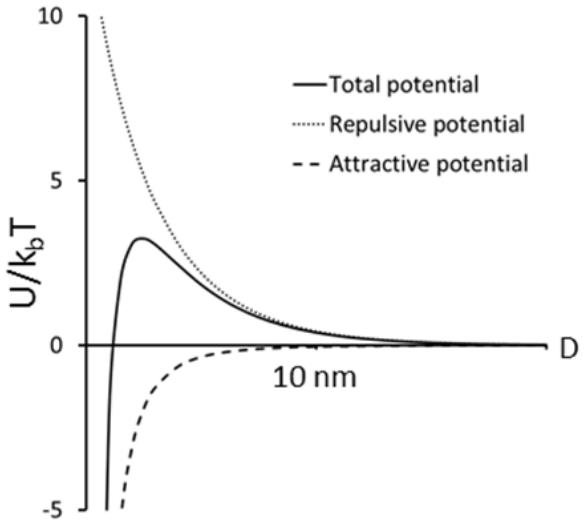

Figure 4.1 Distance dependent interaction potentials in accordance with DLVO-theory. The solid line is the sum of the attractive Van der Waals interactions and repulsive double layer interactions.

The interaction potential is commonly scaled to thermal energy, k_bT, where k_b is the Boltzman constant and T is the temperature. For considerations regarding particle stability, this scaling is highly relevant since the kinetic energy of

approaching particles will be in the same range. Thus, it can be intuitively understood that in order to obtain particle stability for longer periods, the peak repulsive potential must exceed a few k_bT. In the following sections, I will discuss in more detail the different contributions to the interaction potential and some implications relevant for the nanoparticles used in the thesis work.

4.2.1 The electrical double-layer

When a surface is immersed in aqueous solution, it usually acquires a net electrical charge. This can be due to protonation/deprotonation of chemical groups at the interface or due to adsorption of ionic species from the bulk onto the surface. In order to preserve electroneutrality of the system, the surface bound charges are counterbalanced by oppositely charged counterions that assemble in the bulk close to the interface. In close proximity to the surface, within a few Å, the specifically adsorbed ions coordinate loosely bound counterions forming the so-called Stern layer. Surrounding the Stern layer is an assembly of counterions and co-ions, which, due to the thermal agitation in the solution, are distributed in a three-dimensional region called the diffuse layer. Together these two layers define the so-called electrical double layer[47] (figure 4.2).

Close to the surface, the concentration of counterions can be very high compared to the concentration in bulk phase (>10M), the exact amount mainly determined by the surface charge density.[75] In contrast, the density distribution of ions in the diffuse layer mainly depends on the ionic strength I (mol/dm^3) of the electrolyte, given by:

$$I = \frac{1}{2}\sum_{i=1}^{n} c_i z_i^2 \qquad \textbf{(eq. 4.1)}$$

where c_i and z_i are the molar concentration and valence of ion i respectively. For a given ionic strength, the characteristic decay length of the double layer, the so-called Debye screening length κ^{-1} (m) can be calculated according to:

$$\kappa^{-1} = \left[\frac{\varepsilon\varepsilon_0 kT}{1000e^2 N_A 2I}\right]^{\frac{1}{2}} \qquad \textbf{(eq. 4.2)}$$

where ε is the relative permittivity, ε_0 is the vacuum permittivity, k is the Boltzman constant, T is the temperature, e is the elementary charge and N_A is the Avogadro number. As seen from eq. 4.2, the double-layer thickness increases monotonically with decreasing ionic strength. In **paper I, III** and **IV** this phenomena was utilized to tune the distance between self-assembled gold nanoparticles on surfaces as will be further discussed in chapter 5.

4.2.2 Repulsive double-layer interactions

When two charged surfaces, e.g. citrate coated gold nanoparticles, approach each other, electrostatic double-layer interactions arise due to overlap of their diffuse double-layers. For similarly charged surfaces, the double-layer overlap gives rise to a repulsive force that originates from increased osmotic pressure in the overlap region. Thus, the more the diffuse layers overlap, i.e. the closer the particles approach each other, the more the repulsive force will increase.

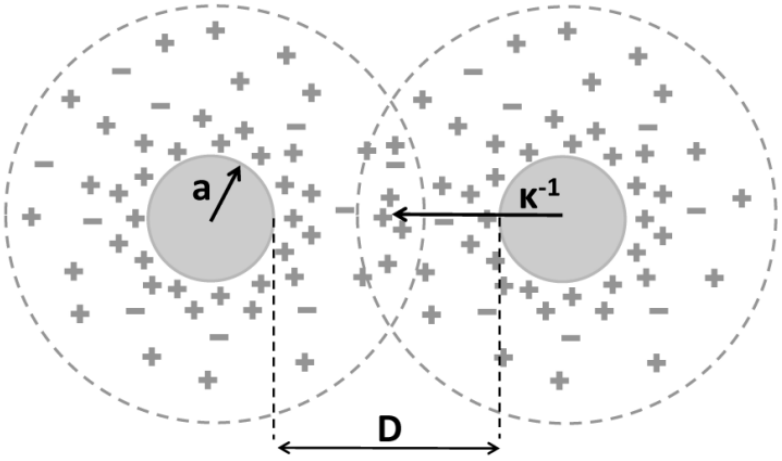

Figure 4.2 Schematic illustration of the double-layer structure surrounding two negatively charged, citrate stabilized gold nanoparticles close to each other. a – particle radius; D – particle separation; κ^{-1} – Debye screening length.

The repulsive interaction potential for two approaching spheres is commonly calculated from the Derjaguin approximation. The applicability of the Derjaguin approximation is however limited to short-range interactions and separations D much less than the radii of the spheres.[75] Therefore, considering the small size of the nanoparticles used in the thesis work, a linear superposition approximation (LSA)[77] was used instead, giving:

$$U_{rep.dl.}(D) = 4\pi a^2 Y^2 \left(\frac{kT}{e}\right)^2 \frac{1}{D+2a} e^{-\kappa D} \quad \textbf{(eq 4.3)}$$

$$Y = 8\tanh\left(\frac{e\psi_0}{4kT}\right) \frac{1}{1+\sqrt{1-\frac{2\kappa a+1}{(\kappa a+1)^2}\tanh^2\left(\frac{e\psi_0}{4kT}\right)}}$$

where Ψ_0 is the surface potential, a is the particle radius, k is the Boltzman constant, T is the temperature and e is the elementary charge. This approximation by Oshima et al. was shown to give accurate results with double layer thickness being in the same range as the particle radius, i.e. $0.1<\kappa a<5$, true for the 10-30 nm nanoparticles used in the thesis work.

4.2.3 Attractive Van der Waals interactions

Irrespective of surface charge, the Van der Waals interactions are always attractive between similar materials.[75] Their origin is the interactions between permanent or induced dipoles in closely positioned bodies. The interactions are commonly divided into three subgroups; the *orientation* interactions due to permanent dipoles, the *induction* interactions due to coupling between permanent dipoles and induced dipoles and finally the interactions between reciprocally induced dipoles, referred to as *dispersion forces*. Out of these three, the dispersion forces are usually the most important. They are quantum mechanical in origin and present between all materials, also electro-neutral, since they rely on dipoles created by instantaneous fluctuations of the electrons about the atom nucleus.

Unlike the double-layer interactions, Van der Waals forces are not (directly) sensitive to electrolyte concentration, surface charge or pH. However, their magnitude differs depending on material, metals having approximately ten times larger interactions than organic matters. The material properties are summarized in the Hamaker constant A_H (J). For interactions across a media, i.e. not vacuum, the Hamaker constant may become retarded for larger separations, which give lower interactions than expected. In the thesis works, Van der Waals

interactions were calculated using the following relation previously used for small gold nanoparticles:[78]

$$U_{attr.VdW} = -\frac{A_H}{6}\left(\frac{2a^2}{r^2-4a^2}+\frac{2a^2}{r^2}+\ln\frac{r^2-4a^2}{r^2}\right) \qquad \textbf{(eq 4.4)}$$

where A_H is the Hamaker constant, a is the particle radius and r is the center to center particle separation (r=D+2a).

4.2.4 Influence of particle size, surface potential and ionic strength

The gold nanoparticles used in the thesis work were electrostatically stabilized by negatively charged citrate ions adsorbed onto the particle surfaces during synthesis. The amount and oxidation state of adsorbed citrate ions cannot be straightforwardly measured. Investigations made on flat gold surfaces (Au(III)) indicates that citrate mainly adsorb as the fully deprotonated citrate ion, C^{3-} for pH>3.[76] However, pH-titration revealed that 10 nm particles quickly aggregated below pH 4 (figure 3.2), which is more in line with the pKa_1 of citric acid (3.13). The citrate ions are very loosely bound to the particle surface, and can easily be replaced by e.g. other ions. It was shown that CO_3^{2-}, $H_2PO_4^{1-}$ and SO_4^{2-} with increasing strength replace citrate,[79] as do most organic molecules, not at least organosulfur compounds.

In order to preserve particle stability and control of the particle surface chemistry, particles were mainly kept in citric buffers with pH≥4. To achieve particle solutions with different ionic strength but similar particle concentration, particles were centrifuged and redispersed in diluted citric buffer with known composition.

To illustrate how electrolyte, surface potential and particle size influence the interaction between approaching particles, DLVO-interaction potentials were calculated as $U_{tot}=U_{attr.}+U_{rep.}$, were $U_{attr.}$ was obtained from eq.4.4 and $U_{rep.}$ from eq.4.3 (figure 4.3). Since the surface charge density was unknown, surface potential could not be determined from the Graham equation.[75] Therefore,

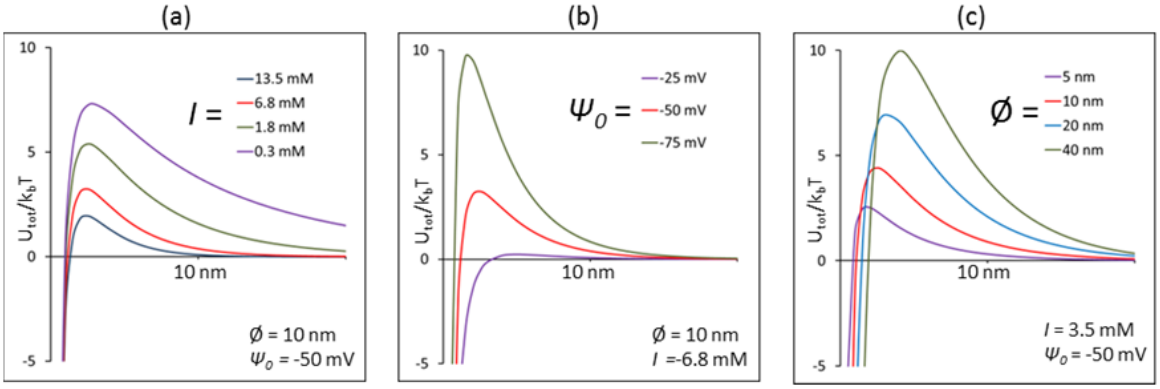

Figure 4.3 Calculated interaction potentials to demonstrate the influence of (**a**) ionic strength, (**b**) surface potential, (**c**) particle size on particle interactions and stability.

calculations were based on experimentally determined ζ-potential values for small citrate stabilized nanoparticles.

The ζ-potential is the potential in the double-layer at the so-called slipping plane some distance outside the Stern-layer. It is experimentally available using e.g. electrophoresis techniques, but always underestimates the real surface potential, i.e. $\Psi_\zeta < \Psi_0$, Nevertheless, ζ-potential values are frequently used to estimate the stability of colloidal dispersions. For citrate capped gold nanoparticles 10-50 nm in diameter, ζ-potential values in the range -25 to -85 mV are commonly found in literature for particle sols with electrolyte concentration <0.1mM. .[78,80] The larger particles tend to have the lower ζ-potentials. For the current modeling, -50 mV was used as reference value for the surface potential and the Hamaker constant was set to 2.5×10^{-19} J.[78].

As seen in figure 4.3a, dilution of the electrolytes increases both the magnitude and range of the repulsive particle interactions. Since also the surface potential will increase for lower ion concentrations, in practice the repulsive potential will increase even more than what is seen in the modeling. Thus, by decreasing the ionic content, particles are effectively stabilized. When surface potential is altered independently of the ionic strength (figure 4.3b) the magnitude of the peak potential shifts drastically. For example, by decreasing the surface potential to -25 mV the repulsive potential is quenched, which can be correlated to the fast aggregation observed for particle solution with pH<4, even though particle stability is very dependent on surface potential, it has *relatively* low effect on the range of the particle interactions.

With increased particle size, the range of the repulsive double-layer interactions increases (figure 4.3c). Thereby, for low ionic strengths, also the range of the total, repulsive interaction potential will increase with particle size. However, also the attractive Van der Waals interactions increase with particle size, which moves the potential peak to larger separations. Consequently, the distance of closest approach before aggregation occurs should be larger for the bigger particles. This behavior could be verified for surface immobilized particles and will be further discussed in the following chapter. As judged from the peak potentials, modeling suggests that larger particles should be more stable than small ones. However, ζ-potential measurements imply that surface potential may be lower for the larger particles. In practice, larger particles are therefore easily aggregated.

5. Self-organization of nanoparticles

In the previous chapter, the stability of nanoparticles in solution was discussed in terms of electrostatic double-layer interactions. These interactions are also active during particle assembly; it is well known that electrolyte concentration can influence the amount of colloids able to adsorb onto a surface. However, somewhat surprisingly, this approach to control particle density has only been utilized to a minor extent for small metallic nanoparticles. Here, I will account for a simplistic model that correlates the amount of adsorbed particles and their relative position on the surface to the electrolyte concentration. I will further give some examples of how this can be implemented to fabricate nanoparticle patterns with some degree of complexity. In **paper III** and **IV**, these nano-patterns were chemically and biochemically modified and used to explore different aspects on cell-adhesion.

5.1 Colloidal assembly

The adsorption of colloidal particles onto solid surfaces is of great practical importance in many industrial processes and biological applications e.g. waste water treatment and chromatographic protein separation. Indeed, early studies on the adsorption of small, micron-sized particles were devoted to such practical issues.[81] Colloidal adsorption was also studied for fundamental reasons, among others as a model for protein and bacterial adhesion. More recently, the formation of two-dimensional arrays of nano-sized particles, in particular metallic, gained interest in the context of electronic and optical devices, catalysis, biosensor applications and functional biointerfaces.[62]

5.1.1 Assembly of polymeric particles in the sub-µm regime

Structuration and ordering phenomena occurring in colloidal dispersions has been recognized for rather long time since these phenomena can easily be

studied in x-ray or light scattering experiments.[82] In contrast, to study particle deposition on surfaces, high magnification imaging techniques are needed. Furthermore, in many early studies on particle adsorption, porous materials were used as collector surfaces. These materials had high relevance for many practical applications; however, the inherent heterogeneities complicated any detailed interpretation of experimental results.[83]

The first to circumvent these practical issues were Adamczyck and colleagues who studied deposition of positively charged micrometer-sized polystyrene latex particles on perfectly flat negatively charged mica sheets using in situ optical microscopy. With theory previously used to describe structure formation in dilute colloid dispersions, Adamczyck was able to both theoretically and experimentally demonstrate the significance of lateral double-layer interactions for irreversible particle adsorption.[84] Using imaging techniques with higher resolution such as AFM (Atomic Force Microscopy), similar experiments were later performed with smaller particles in the range 50-200 nm in diameter. Several investigators studied the effect of particle size, size-distribution, different substrates, pH and electrolyte concentrations on particle binding.[80,82,8385] Also in these studies, a main correlation was found between interparticle distance and the ionic strength in the particle solution, a correlation that became more prominent for the smallest particles.[83,86,87]

Besides its importance for the fundamental understanding of particle adsorption phenomena, adsorption of polymeric particles has also come into practical use for nano-lithographic processing.[88] Self-organized polymeric particles, mainly in the range 50nm to 1μm, are frequently used as sacrificial masks for lithographic fabrication of optical devices[89], sensor surfaces[90] and biofunctional interfaces[91,92]. By variations of such *colloidal lithography*, different structures like dots, pits, holes, rings etc. may be implemented on relatively large surfaces.

5.1.2 Assembly of small metallic nanoparticles

Sterically stabilized metallic nanoparticles (predominately gold nanoparticles <15 nm), for example thiol-stabilized particles[93-95] or particles encapsulated in block copolymers[96-99] can easily be organized into highly ordered superlattices. This assembly is however not entirely spontaneous, but enforced by capillary

forces during solvent evaporation or by electrophoretic forces[100]. Normally, the interparticle distance is controlled by the size of the stabilizing ligand and evaporation kinetics[101,102], which results in very reproducible but less flexible patterns. Since particles are transferred to non-binding substrates, these nanoparticle patterns can be sensitive and difficult to use as they are. For certain applications, nanoparticles can however be firmly fixated on the substrate by plasma-treatment subsequent to the assembly[98].

From a practical point of view, a more flexible and straightforward approach to two-dimensional gold nanoparticle arrays is the irreversible, spontaneous binding of charge-stabilized particles to surfaces. This proceeds in analogy with the adsorption of polymeric particles to oppositely charged surfaces described above. Instead of natively charged materials, substrates are usually chemically modified with SAMs that provide a strong binding, e.g. glass/silicon modified with amino-presenting silanes like 3-aminopropyltriethoxysilane (APTES) or thiol-presenting silanes like 3-mercaptopropyltrimethoxysilane (MPTMS). Both amines and thiols are known to form strong, covalent-like bonds to gold nanoparticles; however, the thiol-bond is stronger and will replace other bound species.[103,104]

The first systematic study aiming to control the assembly of citrate stabilized gold nanoparticles was published in 1995 by Grabar and colleagues[39]. They investigated binding of gold nanoparticles, 12-15 nm in diameter, to silicon dioxide surfaces treated with different silanes and found that especially MPTMS adsorbed the nanoparticles very efficiently. Early on in the adsorption, sticking probability was approaching unity, indicating that virtually all particle-surface collisions lead to particle immobilization. They also noted that electrostatic repulsion between the negatively charged particles slowed down the adsorption, giving a saturated layer with sub-monolayer coverage.[40] However, no systematic variation of electrolyte concentration was undertaken in order to control particle spacing, instead it was suggested that particle coverage could be controlled by variation of immersion time

Indeed, variation of particle concentration or time for particle assembly is the most common strategy to achieve sub-monolayer coatings of gold nanoparticles.[62] Another increasingly popular approach is molecular patterning, where gold-binding molecules (commonly amines) are mixed with non-binding

molecules.[105] However, generally both approaches give low control of nanoparticle organization and low reproducibility, partly since effects of lateral electrostatic interaction between adsorbing particles has been neglected. This was first highlighted in the works by Kooij and colleagues, who produced a follow-up study with the same surfaces, molecules and particles as Grabar.[106] By systematic variation of the ionic strength they were able to reproduce the similar lateral ordering phenomena as described by Adamczyck and others for larger polymer particles.

The experiments reported in **paper I** are closely related to those of Kooij et al., with the important exception that octanedithiol modified gold was used as substrate instead of APTES coated silicon dioxide surfaces. Compared to the silane treated surfaces, the dithiol modified gold surfaces were shown to bind gold nanoparticles with increased ordering and dynamic range. Apparently, the stability of the obtained patterns also increased, probably relating to the superior ordering and reactivity of the dithiol self-assembled monolayer.

5.2 Role of electrostatic interactions in particle assembly

The most widely used model of adsorption is Langmuir's equation for reversible molecular adsorption, which accounts for the exclusion of mutually independent binding sites on a substrate.[107] In contrast to adsorption of small molecules, which ideally occurs at discrete sites on the substrate, the larger colloidal particles interact over longer distances giving rise to complex surface exclusion effects. Furthermore, colloidal adsorption is more or less always irreversible. Thus, the Langmuir adsorption model provides a rather insufficient description of particle adsorption. Instead, a more appropriate description of particle adsorption can be derived from the theoretical model for random sequential adsorption (RSA).[108]

5.2.1 Random sequential adsorption of interacting particles

Random sequential adsorption assumes that particles are placed one by one at random locations on a surface with uniform binding affinity. In the case of hard particles, each placement yields an irreversible and fixated particle unless the particle does not overlap with another already bound particle. If so, the

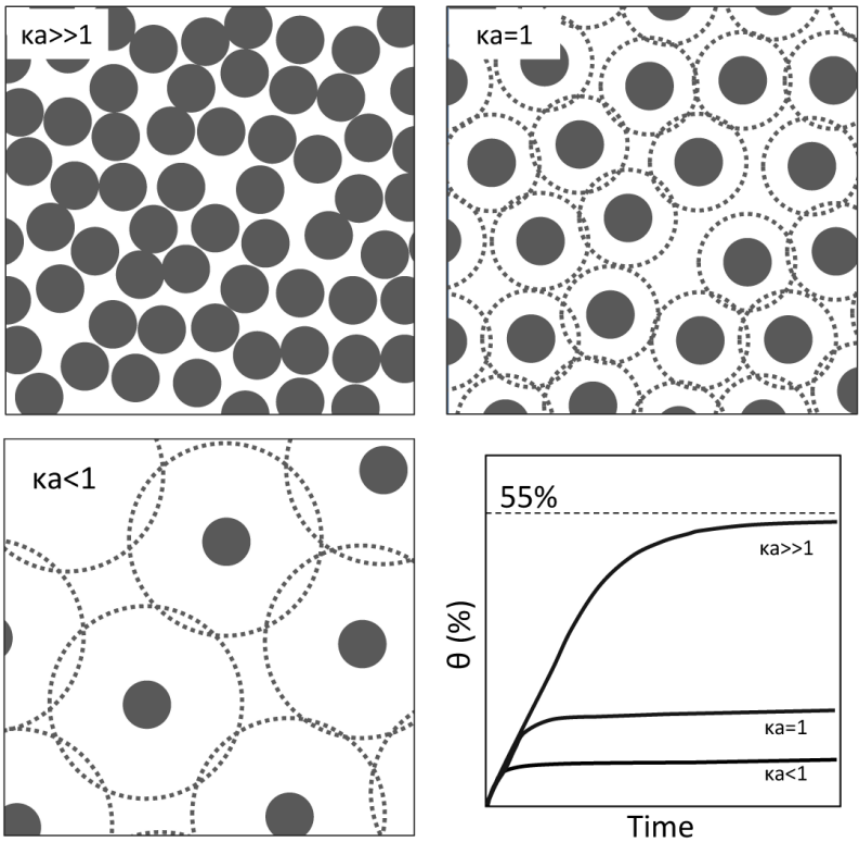

Figure 5.1 Schematic illustration of randomly adsorbed particles deposited at different conditions defined by the screening parameter *κa*. For *κa*≤1, the double-layer exceeds the hard core radius, thus acting as a soft shell surrounding the particles. Characteristic curves describing the random sequential adsorption process are presented in the lower right corner.

placement is unsuccessful and the particle disappears from the surface. The maximum surface coverage that can be obtained by a RSA process is 54.7% given that all objects are perfectly spherical, have the same size and only interact via their hard surfaces (figure 5.1). Initially all particles that reach the surface will bind and the early adsorption will therefore be limited by the diffusion of particles to the surface. Many studies show, that initially particle adsorption is a first-order rate process with respect to the particle concentration.[40,83,84,86,87] As the surface coverage increases and exclusion effects become important, the deposition rate quickly decreases and saturation coverage will be reached in the limit of long times.

As demonstrated in several studies, also particles interacting via double-layer repulsion were seen to assemble onto surfaces in accordance with the RSA process. However, according to the model introduced by Adamczyck, because

of the electrical double-layers these particles should be treated as soft spheres with hard cores, rather than purely hard particles.[84] With decreasing ionic strength, the Debye length (κ^{-1}) increases and the distance of closest approach between particles will increase as well. Within the RSA approximation, increased long-range interactions are equivalent with a thicker soft shell around each particle. Thus, deposition at low ionic strength will give rise to saturation coverage well below the theoretical jamming limit of 55%. This effect is most relevant for the smallest nanometer-sized particles, i.e. $\kappa a \leq 1$ (a is the particle radius) whereas it becomes negligible for larger micrometer-sized particles, i.e. $\kappa a >> 1$, where the hard core exclusion effects dominate.

5.2.2 The hard-sphere approximation

In order to estimate the range of the "soft" particle interactions on the surface, a straightforward approach is to assign an effective hard sphere radius, a_{eff}. to each particle (figure 5.2).

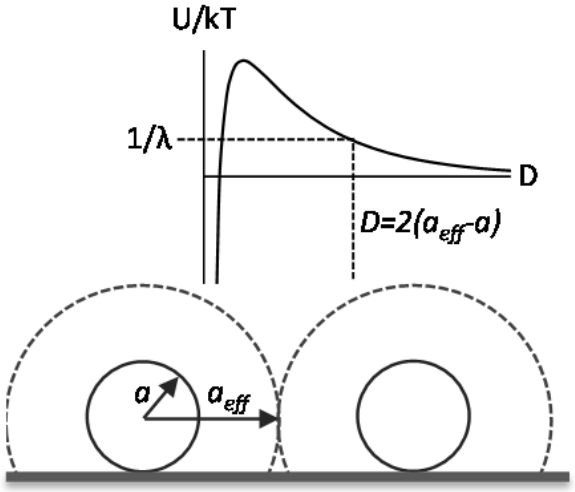

Figure 5.2 Schematic that illustrates how an effective hard sphere radius a_{eff}. can be estimated from the particle pair potential.

The effective radius is then correlated to the particle interaction by an effective threshold potential so:

$$\frac{U_{pp}(2a_{eff})}{kT} = \frac{1}{\lambda} \qquad \textbf{(eq. 5.1)}$$

where $U_{pp}(r)$ is the pairwise particle interaction potential, kT the thermal energy and λ is a constant $1<\lambda<e$.[82] The pairwise interaction potential can be obtained from the repulsive and attractive interaction potentials calculated from eq. 4.3 and eq. 4.4 respectively. By numerical solvation, $a_{eff.}$ can be obtained from eq. 5.1 and further used to estimate the saturation surface coverage by the geometrical scaling:

$$\theta = \theta_{jam}\left(\frac{a}{a_{eff}}\right)^2 \qquad \textbf{(eq. 5.2)}$$

where θ_{jam} = 0.547 is the surface coverage at the saturation limit for RSA of hard spheres.

The above outlined model has been used by many investigators to evaluate Debye-screening controlled particle spreading on surfaces[86,106] and was also successfully used to describe the spreading of 10 nm gold nanoparticles in **paper I.** The model offers some degrees of freedom since virtually both the surface potential (or surface charge) and the threshold potential cannot be absolutely determined. Apparently, depending on the specific particles and surfaces used, to acquire a good fit between experimental and modeled data, different authors have used different values of the constant λ. For example, in the thesis works λ=(e-1)/2 was used, whereas Adamczyck used λ=1[84], Semmler used λ=e[86] and Kooij used λ=2/3[106]. In all cases, within the same set of data the model could well describe the effect of electrolyte concentration on particle separation and surface coverage.

It should be mentioned that also other, more elaborate, approaches to model nanoparticle assembly exist. Most important, several Brownian dynamics simulations (BDS) have been performed.[109-112] In these simulations, the force imparted on the colloidal particle is computed as the sum of the deterministic interparticle and particle-surface forces and the stochastic Brownian forces imparted by the solvent molecules. Compared to the classical RSA-model, here particles are not positioned one by one in sequence, but several particles can be positioned at the same time and in dependence of each other. Furthermore, the RSA-model does not consider transport of particles beyond distances comparable to the particle diameter from the surface. In contrast, in the

computational modeling, the dynamics of all particles in the simulation box are considered.

Interestingly, these simulations show that irrespective if particles can move laterally on the surface[109] or if they are fixated at the position where they first adsorb[111,112], the ordering among the bound particles will increase with lower *κa*. In **paper I**, binding of 10 nm nanoparticles onto dithiol modified gold surfaces was investigated. Since these particles were small, *κa*<2 for all possible electrolyte concentrations. Thus, these specific results from simulations are highly relevant for the experiments on nanoparticle binding in **paper I**.

5.2.3 Two-dimensional radial distribution functions

To access statistically relevant information about particle separation and particle ordering from e.g. electron microscopy micrographs, a two-dimensional radial

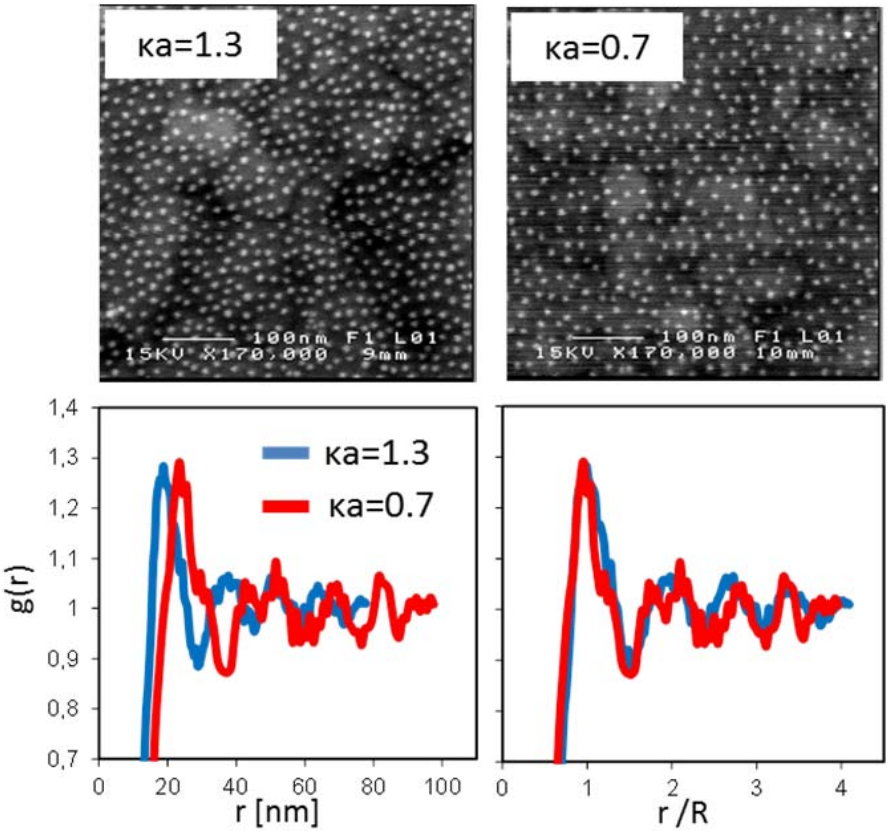

Figure 5.3 Two-dimensional radial distributions calculated for 10 nm gold nanoparticles assembled onto dithiol modified gold substrates for two different *κa*. In the lower right graph, radial distributions were scaled by the average particle separation *R*.

distribution function can be generated.[81] The radial distribution function *g(r)* expresses the local surface concentration of particle centers at a separation *r* normalized by the average surface concentration (figure 5.3).

In the thesis works, radial distributions were determined from SEM micrographs using a Matlab subroutine (available in Appendix A). In figure 5.3, radial distributions for 10 nm gold nanoparticles deposited onto dithiol modified gold substrates at two different ionic strengths (κa=1.3 and κa=0.7) are presented. The first larger peak in the radial distribution gives the average particle separation *R* and its presence indicates a short range ordering among the particles. However, several smaller peaks can also be seen at larger separations, which is indicative of a certain degree of long-range order. By scaling the particle separation with *R,* distributions for different κa collapse into a single curve indicating that both distributions originate from the same process.

Interestingly, the observed radial distributions are close to those determined by BDS for particle deposition at low κa where periodic oscillations can be seen up to 5R.[111] The increased particle ordering at low κa reflects an increased impact of soft double-layer interactions and decrease of hard geometrical surface exclusion effects. This can clearly be seen by comparison of radial distribution for κa=1.84, giving the closest packing possible of 10 nm gold nanoparticles before aggregation occurs, and κa=0.7, which gives a particle separation of approximately 15 nm. For the surfaces with higher particle coverage, a distinct primary peak can be seen in the radial distribution, however no or very weak periodic oscillations can be seen. In contrast, for the surface with low surface

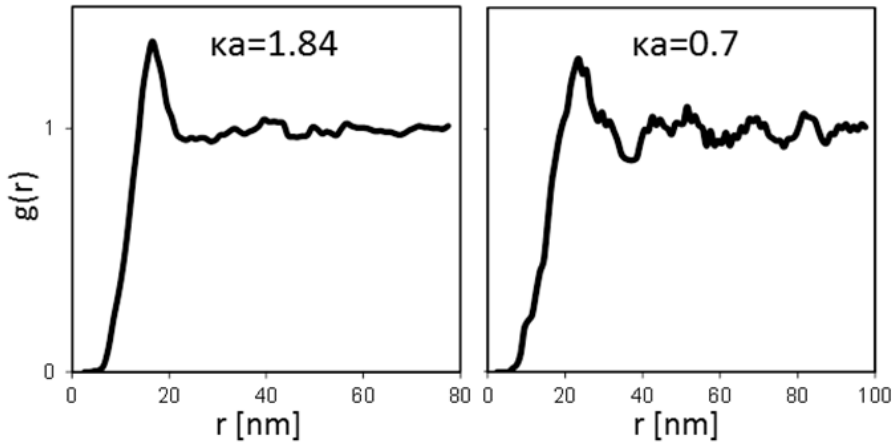

Figure 5.4 Two-dimensional radial distributions calculated for 10 nm gold nanoparticles assembled onto dithiol modified gold substrates for two different κa.

coverage, the primary peak is less distinct; however, periodic oscillations are clearly visible. These observations are also in line with BDS results.

It is notable that the periodic oscillations observed here are more pronounced than commonly seen for larger polymeric particles assembled at low *κa*. This may be due to some experimental artifacts appearing more easily for the larger particles. Firstly, to obtain low *κa* for larger particles requires lower ionic strengths than for smaller particles. This can be hard to obtain for practical reasons as well as making the system very sensitive to contamination. Secondly, it is often reported that adsorbed polymeric particles are sensitive to capillary forces and can move on the surface due to drying procedures[87,88], which of course effects the measured radial distributions.

In contrast, the gold nanoparticles bound on the dithiol layers appear to be very well fixated in position and do not show any tendencies to lateral movements on the surface. Moreover, compared to earlier results obtained for small gold nanoparticles bound to thiol- and aminosilane modified surfaces[40,106], the increased quality of the nanoparticle layers can be interpreted as an effect of the homogenously organized supporting dithiol monolayer. A homogenous supporting layer will not impose any "unorder" among the adsorbed particles, but may also provide more binding points for each particle, giving an increase in overall affinity and bonding strength.

6. Electrostatic design of nanopatterns

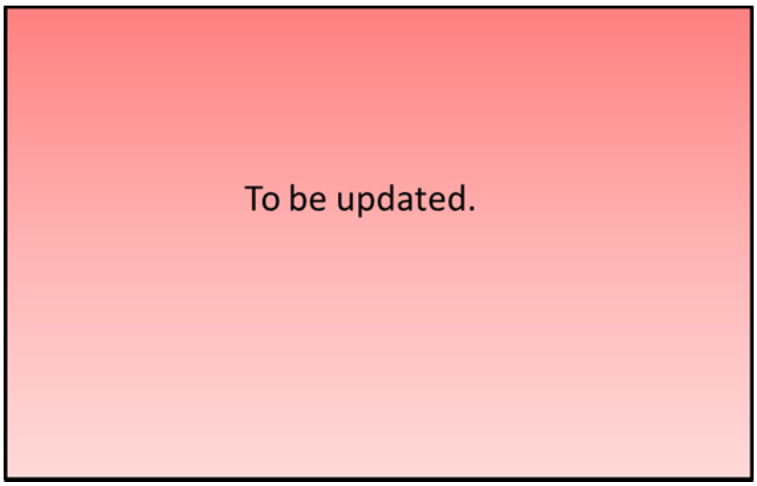

6.1 Backfilling with nanoparticles

6.2 Gradient nanoparticles

7. Biofunctional interfaces

Biofunctional interfaces are surfaces or scaffolds designed to interact with a biological milieu in a predictable, desired manner. These interfaces can be applied within the context of biomaterials, tissue-engineering, regenerative medicine and cell-culture with the aim to control the functionality of adhered tissue-cells.[5,89] As an example of other applications, surfaces can also be designed to withstand adhesion or growth of bacteria, thereby minimizing transmission of infections or heavily fouling due to bacterial films in industrial processes.

With few exceptions, interactions between tissue-cells and their surrounding is mediated by proteins. This can be specific interaction between receptors on the cell surfaces (integrins) and specific ligands, commonly adhesive proteins or proteoglycans (sugars).[1] These types of interactions dominate in natural systems and are responsible for the fine-tuned organization of cells into tissue. On man-made surfaces like implantable biomaterials, cell-interactions are mainly directed by proteins nonspecifically adsorbed onto the surfaces from solution, e.g. blood, or by secondarily bound proteins excreted by the cells themselves.[113] Given this, designing biofunctional surfaces is much about controlling and directing protein binding.

7.1 Approaches to controlling cell-surface interactions

7.1.1 Protein coatings

A key starting point for the design of biofunctional materials is to functionalize surfaces with factors that promote the adhesion and survival of selected cell types. Three main strategies to construct these surface cues can be pointed out in the literature. The first and most fundamental method is adsorption of ECM-

proteins on cell culture substrates. This approach is advantageous in that all biological information encoded in the primary protein sequence is preserved.

However, drawbacks associated with protein adsorption is low control of surface concentration and ligand spreading, or the loss of signaling function due to unfavorable surface interactions or conformational changes. The influence of surface interactions on protein conformation and bioactivity can be tuned by the chemical composition of the interface[114], as well as by the use of specific, chemical or biochemical protein coupling techniques.[115]

The by far most investigated protein is the multiadhesive ECM-protein fibronectin. Besides epitopes that mediate various integrin binding, fibronectin also has binding sites for many other components of the ECM, e.g. heparin, collagen and fibrin(ogen), which is a major part of blood-clotting and also serves as a provisional cell-matrix during wound-healing. Fibronectin is also present in blood plasma, however in a closed inactive form, able to become active upon surface immobilization or binding to fibrin.[1]

Fibronectin plays a key role in cell adhesion and has also been correlated to cell differentiation *in vitro* [116]and normal embryogenesis *in vivo*.[117] It is also one of the first proteins that cells produce and secrete after surface binding has been established.[1] In addition to fibronectin, also other ECM-proteins such as laminines[118,119] and osteopontin[120,121] have been explored as bioactive surface coatings. Collagen, a major constituent of the ECM, assembles into fibers and has mainly gained attention in the context of three-dimensional scaffolds.[122] The same is true for fibrinogen, which can be turned into fibrin scaffolds by reaction with thrombin. [123]

7.1.2 Cell-signaling peptides

To control topographical presentation of surface ligands, surface patterns can be engineered to allow a certain amount of ligand to be presented on an inert background.[89,124] These micro- and nano-patterns have commonly been fabricated on silicon surfaces using lithographic techniques such as dip-pen lithography[125], colloidal lithography[91,92], or block copolymer micelle nanolithography[98]. Patterns may be site-specifically modified with

proteins[91,126,127], or commonly with shorter peptides that have been found to mediate cell-interactions.[128,129] A well-known example is the RGD-peptide (RGD is short for the amino acid sequence Arginine-Glycine-Aspartic acid), an integrin-binding domain present within adhesive ECM-proteins such as fibronectin, vitronectin and osteopontin, some laminines, collagens and fibrinogen.[1]

Compared to native proteins, the use of peptides offers several advantages.[130] For example, peptides can be straightforwardly synthesized at low cost, and their use also lowers the risk for immune reactivity and pathogen transfer compared to native proteins from cadaveric protein sources. Furthermore, many short signaling and adhesive peptides are recognized by the cell as a primary amino acid sequence[1], although peptide conformation to different extent can modulate affinity[131,132]. Thus, peptides are generally less sensitive to surface interactions and can also be maintained throughout sterilization processes, which would normally cause protein denaturation.

Even though engineered substrates offer high control of the spatial distribution and presentation of ligands, concerns may be raised that these patterns contain too little biological information compared to native proteins.[133] Indeed, co-immobilization of RGD with the peptide PHSRN, also from fibronectin, indicated important synergistic signaling effects.[134]

Similarly, as demonstrated and further discussed in **paper IV**, RGD co-immobilized with biologically active heparin increased cellular motility and interactions compared to RGD presented on a background of inert poly(ethylene glycol) (PEG). Thus, the use of RGD-peptides alone may represent a too large oversimplification to serve as a general replacement of native proteins. Improvement of patterning technology, allowing organization of multiple functionalities may however enable realization of patterns displaying a higher biological complexity.

7.1.3 Morphological stimuli of cells

A third approach to modulate cell function is to introduce morphological cues, e.g. nano-sized pillars on cell culture substrates.[135,136] Morphological features are frequently seen to have a significant effect on both proliferation and

differentiation of adhering cells. The most commonly observed trends are that cell differentiation and the synthesis of extracellular components increase with increased surface roughness and disorder.[113] Interestingly, in contrast surfaces displaying very ordered structures, such as hexagonally arranged pits in 100-nm range, were recently shown to impair cell differentiation. Actually, cells on such

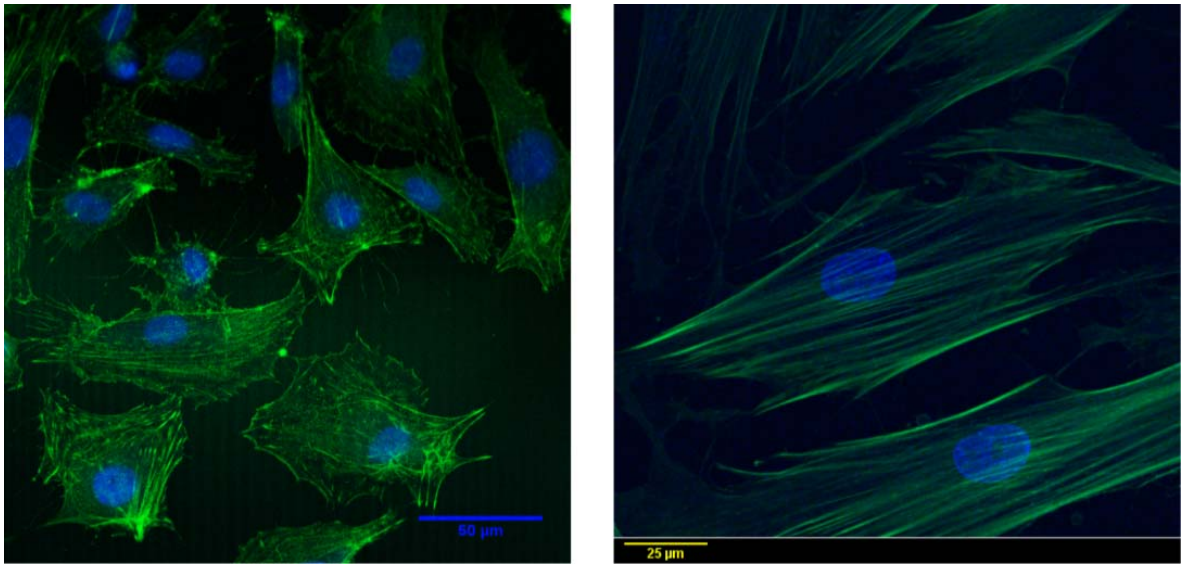

Figur 7.1 Confocal laser scanning microscopy (CLSM) pictures of cells studied in the thesis project. (Left) Primary human vascular endothelial cells (HUVEC) grown on a monolayer of carboxylated G4 dendriners as detailed in **Paper III**. (Right) Normal human dermal fibroblasts grown on a nanopatterned surface modified with fibronectin and poly(ethylene glycol) as detailed in **Paper IV**. Nucleus were stained with DAPI (blue) and actine filaments were stained with phalloidin (green)

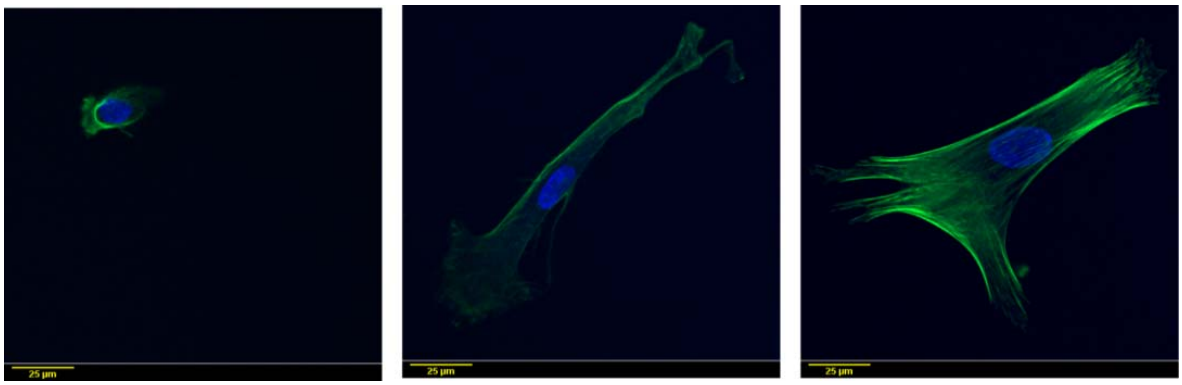

Figure 7.2 CLSM pictures of normal human dermal fibroblasts studied grown on a nanoparticle gradient surface modified with cell-binding RGD peptides and poly(ethylene glycol) (Left) Undeveloped, round cell from a position on the gradient with low RGD concentration. (Center) Polarized cell from the central part of the RGD-gradient surface were the RGD-concentration continuously increases. (Right) More spread cell from the plateau of the gradient surface where RGD concentration is high.

surfaces were put on "stand-by" mode with reduced metabolic activity.[7] These effects are thought to be due to mechanical sensing mechanisms of the cell as a response to restriction in binding possibilities. It can be speculated that surfaces with morphological features to some extent mimic the three-dimensional microenvironment of cells that is found *in vivo*, with among other things an increased supply of nutrients etc. However, the strong effect of order/disorder on cell differentiation will need more consideration to be fully understood.

Recent reports also state that protein adsorption and presentation can be very different on nano-topographic features compared to flat surfaces. A general trend, mainly obtained from studies on interactions between proteins and nanoparticles in solution, is that increased curvature reduces the amount of conformational changes that proteins undergo upon adsorption.[137,138] Most studies were however made on small globular proteins. In contrast, the larger and structurally unstable fibrinogen underwent large conformational changes when adsorbed on small nanoparticles.[139] It was also shown that even soft interactions between enzymes and nanoparticles could alter enzyme functionality and the tertiary structure of the enzyme in dependence of the particle size.[140]

In **paper II,** we explored the hypothesis that gold nanoparticles adsorbed to and sintered into a surface would affect the surface activation of the innate immune response, i.e. the complement protein cascade system. It was found that the presence of nano-topography strongly attenuated the complement activation on surfaces incubated in blood serum; however, this effect was dependent on surface chemistry since hydrophobization of nanostructured surfaces led to strong complement activation.

This observation was further supported by investigations on the protein corona of polymeric nanoparticles incubated in plasma by Lundqvist and colleagues[141], who found that some complement proteins were absent on hydrophilic but present on hydrophobic particles of similar size. Thus, these results imply that the combination of mechanical and altered biochemical stimuli ought to be considered when cell responses to non-flat substrates are evaluated.

7.1.4 Surfaces organized at nanolevel

Regardless of methodological approach, surface signaling has proven to be efficient in modulating cell function, e.g. to control stem cell proliferation[7,136,142] or to reveal fundamental aspects of cell adhesion.[8,127] This development has been governed by the progress within nano-fabrication methodology, and it is likely that further advancements will be readily realized given that the tools for organizing substrates in the appropriate regime become more generally available.

The use of nanoscopically modified surfaces for exploration of cellular functions has been successful, the main reason being the fact that nanoscopic features can be made in the size of proteins, or clusters of proteins, working as functional units in cells. Thus, such features allow a direct cross talk with cells at the most fundamental level. This of course also facilitates development and testing of more exact hypotheses, which earlier could not be done due to low control of the amount, distribution, direction and co-localization of surface bound species.

A specific aim of this thesis was to demonstrate the feasibility of the direct nanoparticle self-organization approach for the assembly of biofunctional interfaces. The nanoparticles used in the thesis works were all in the size-regime 5-50 nm in diameter, which is approximately the same size as most proteins and many other macromolecules. Thus, these gold nanoparticle decorated surfaces should be well suited for addressing hypotheses regarding biological binding at protein level. Furthermore, the dithiol surface modification provides an excellent stability of the bound gold nanoparticles; e.g., no reorganization of nanoparticles could be seen due to capillary forces induced by drying, which is frequently observed for polymer particles.[87]

In **papers II-IV**, in addition to the already discussed approaches to particle self-organization, the modification of nanoparticle patterns using surface chemical approaches was investigated. In consecutive order, nanoparticle patterns were modified to achieve different nanoscopic compartments (figure 7.3):

(i) Surfaces with nanostructure, but homogenous (gold) chemistry, the size and number of nanoscopic protrusions determined by particle size and number.

(ii) Surfaces where nanoparticles were site-specifically modified with molecular binders, e.g. proteins, on an inert chemical background, allowing control of number and distance between possible binding points.

(iii) Surfaces where areas between nanoparticles were site-specifically modified with molecular binders, whereas particles were made inert, allowing the size of the binding domains to be controlled by particle separation.

Figure 7.3 Schematic illustrations of the three types of nanopatterns that were created in the theses works. **(Left)** Surfaces with nanostructures and homogenous chemistry. **(Center)** Surfaces with adhesive particles and inert surroundings. **(Right)** Surfaces with inert particles and adhesive surroundings.

Sintering of gold nanoparticles into the gold substrate could trivially be achieved by immersion of surfaces in an oxidizing bath and gentle heating. To facilitate the removal of thiols from the gold substrates, water-soluble cysteamine was however used to assemble the nanoparticles instead of octanedithiol. The site-specific modifications used for the assembly of the other patterns involve some more elaborate procedures, e.g. protein adsorption and coupling, as discussed in the following section.

7.2 Site-specific chemical modifications

7.2.1 Protein adsorption

The assembly of proteins at an interface is both a trivial and very complex issue. Trivial since most interfaces efficiently adsorb proteins from solution, but complex since interactions between the surface and adsorbed proteins may hamper protein function.[143,144] Compared to other molecules, proteins are very complex in the way of their functionality being intimately coupled to their

conformation, i.e. structure. The three-dimensional protein structure is a result of an intricate folding of the primary amino acid chain, where hydrophobic amino acids primarily ends up in the central core of the proteins surrounded by hydrophilic, water binding amino acids. (This is only true for water-soluble proteins; membrane-penetrating proteins will expose hydrophobic amino acids on their surface.)[145]

Thus, protein folding is mainly driven by the gain in entropy as water ordered around non-polar amino acids is released when these aggregate. However, this gain of entropy is partly counter-balanced by the loss in configurational entropy of the polypeptide chain itself. In the end, protein stability and exact conformation thus often rely on the cooperative effects of many other, weak intramolecular interactions such as hydrogen bonds between different amino acids[145], which can easily be disturbed by surface interactions.

There is no straightforward theoretical or experimental approach fully encompassing the process of protein assembly at an interface. This is partly due to the inherent complexity of the protein, i.e. the large number of atoms and possible interactions with the surface. It is also due to the interplay between adsorbed proteins and protein in solution[144,146], this being especially prominent in biological solutions such as blood, plasma, serum etc.[147] From experiments, it stands clear that the outcome of an adsorption process depends on many factors such as chemical composition and structure of the interface, concentration, size and type of involved proteins and solution parameters like ionic content, pH and adsorption time.[143] From a systemic point of view, adsorption will be governed by:

(i) Change in free energy due to interactions between the protein and the surface, interactions between proteins or interactions within proteins.
(ii) Change in free energy due to surface dehydration.
(iii) Change in free energy due to release of water from proteins and recovery of hydrogen bonds among water molecules.

The relative impact of these factors is debated.[148] One view states that protein adsorption is very little dependent on molecule-specific interactions (category i), and that all proteins are approximately similar. Instead, protein adsorption is a very dynamic process, mainly determined by displacement of water from

surfaces (category ii), protein size and protein concentration in solution (category iii). From another point of view, protein adsorption is more dependent on protein interactions with the surface (category i), and the outcome of adsorption, i.e. which proteins are found on the surface after adsorption, is mainly dependent on variations in the protein structure.

There are some good arguments suggesting that for the combination of hydrophilic surfaces and complex protein solutions, the dynamic model will dominate. However, as surface hydrophobicity increases, the influence of the surface interactions increases as well. Undoubtedly, at single protein level, specific interactions between protein and surfaces cannot be neglected. For example, the bioactivity of many ECM-proteins[149] and provisional interim matrix proteins like fibrinogen[150,151] is largely governed by their structural conformation.

When adsorbed on methylated (hydrophobic) surfaces, fibrinogen undergoes substantial conformational changes increasing the cell binding activity of the protein.[152] In contrast, fibronectin attains a globular biologically less active conformation on hydrophobic surfaces[153,154], but the activity can be preserved by other surface chemistries and immobilization methods giving a flat and extended protein structure similar to native fibronectin in the ECM[115].

7.2.2 Orthogonal chemistry

For the assembly of functional nanopatterns, besides the control of lateral organization, ultimately also surface chemistry must be site-specifically adaptable. For these purposes, the usage of highly specific chemical modifications, which can be utilized to firmly immobilize functional components, e.g. proteins, is necessary. Such methods are often referred to as “orthogonal modifications” or “orthogonal chemistry”, and mainly rely on different organic chemical reactions to form covalent interactions between the binding partners.[38]

For bottom-up modification of inorganic surfaces, as detailed in chapter 2, modification of gold with functional thiols and oxides with silane chemistry are common methods. For conjugation of macromolecules, popular approaches

include the use of maleimides to bind free sulfhydryls and (EDC/NHS) (ethyl(dimethylaminopropyl) carbodiimide/N-Hydroxysuccinimide) to interconnect (form a peptide bond) primary amines and carboxylic acids.

The high affinity biospecific binding between biotin and the protein streptavidin is also often utilized. Streptavidin is then working as a linker between two biotinylated binding partners, e.g. a surface and a protein. A less specific, however common approach is to use electrostatic interaction between oppositely (highly) charged species such as amine carrying polymers and negatively charged surfaces or vice versa.

To achieve site-specific modifications on nanopatterned surfaces, chemical modifications are chosen with respect to the chemistry of nanostructures and background respectively. For lithographically processed patterns, nanostructures have mainly been fabricated in gold on a background of oxide material. Thus, thiols could be used to functionalize nanostructures whereas silanes or electrostatic approaches dominate for the modification of background surfaces.

For the self-organized gold nanoparticle templates used in the thesis works, thiols were used to modify particle surfaces, whereas surrounding areas were modified via grafting of maleimide conjugates to free sulfhydryls in the dithiol SAM. This way, different complementary functionalities, e.g. inert poly(ethylene glycol), hydrophobic non-polar methyl-groups or biotin could be presented on particles and surrounding areas respectively.

7.2.3 Protein resistant modifications

Since proteins strongly tend to accumulate at interfaces, the possibility to introduce chemical modifications that can resist protein binding is of great importance for many applications. Research on protein resistant coatings has been an ongoing topic within surface science for several decades. A large portion of work was done in the context of blood-contacting surfaces[155], with the aim to minimize surface induced blood coagulation and thrombogenicity, intimately connected to the adsorption of certain proteins, e.g. fibrinogen.

So far, despite all efforts few surface modifications have been developed able to successfully withstand protein adsorption. This is understandable considering the large internal heterogeneity of the protein molecules and the structural and chemical variability between different proteins. Even though a surface coating can be designed for rejecting a certain protein efficiently, it is much more difficult to design a coating that rejects all kinds of proteins.

Among those few modifications that do withstand protein adsorption, introduction of poly(ethylene glycol), PEG, on surfaces is the most common approach. The efficiency of PEG for resisting protein adsorption when grafted to surfaces was demonstrated in the early 1980s[155], and has ever since been the first choice for applications where high protein resistance is required. PEG, which frequently also is referred to as poly(ethylene oxide), PEO, is a water soluble and uncharged polymer that interacts strongly with water molecules via hydrogen bonds to oxygen in the polymer backbone.[156]

The protein repulsive properties of PEG was originally explained as an effect of steric repulsion from the large excluded volume of the mobile PEG-chains, which resulted in unfavorable compression and restriction of polymer segments upon approach of a protein.[157,158] These ideas were supported by experimental results showing that protein resistance increased with the length and density of grafted PEG molecules.[159] Nevertheless, more recent experiments clearly demonstrated that very high protein resistance also could be obtained with shorter, although well-organized oligo(ethylene glycols), indicating that other effects but steric repulsion are needed to fully explain the protein repelling effect.[160]

Thus, contemporary research relates the protein repulsive properties of PEG mainly to its ability to strongly bind and organize water in its vicinity.[161] Nevertheless, from a practical point of view, the PEG-chain lengths as well as the grafting density on surface are both important parameters when it comes to the realization of effective PEG-coatings. A drawback of PEG is its poor stability; the molecule is sensitive to oxidative degradation[162] and can also be digested by some bacteria.[163]

Besides PEG, other types of modifications that showed good or moderate protein resistance include surface grafting of polysaccharides or even

monomeric or dimeric sugars. Best known is probably the glucose-based polysaccharide Dextran[164], successfully used as a coating of biosensor surfaces. In the context of surfaces aimed for the study of cell interactions, it should be remembered that many sugars and polysaccharides naturally are found at the surfaces of cells, strongly interacting with some proteins.[1] Thus, polysaccharides like for example heparin might repulse most proteins, but will bind strongly to fibronectin and many growth factors[165].

Another class of protein repulsive materials that lately received some attention is zwitterionic and charge balanced materials, containing equal amounts of closely positioned positively and negatively charged chemical groups.[166] As for PEG, these materials are strongly hydrated, which may explain the protein resistance effect. In contrast to PEG, zwitterionic molecules can be found in the nature, the phosphorylcholine lipid head group found in some cell membranes being a prominent example[1].

Supported lipid bilayers made from these lipids were shown to be protein resistant; an effect which in addition to the zwitterionic character of the lipid head groups, also may be governed by the lateral movements of lipids within the bilayer.[167] Recently, a supported lipid bilayer was used to coat glass surfaces surrounding nanosized dots of gold on a nanopatterned surface.[129]

7.2.4 Site-specific grafting of poly(ethylene glycol)

For site-specific modifications of nanosized features with proteins, the efficiency of the protein resistant coating covering surrounding areas must be very high, since those areas can be very large compared to the area of the features that should be modified. For nanopatterns fabricated on substrates of glass or silicon dioxide, PEG molecules have been grafted to these surfaces using silane chemistry.[168] An alternative, very popular route to introduce PEG is the use of the positively charged polymer poly(L-lysine) with PEG-chains grafted to its backbone, forming the co-polymer PLL-g-PEG. On oxide-covered surfaces having a native negative charge at neutral pH, PLL-g-PEG adsorbs with the positive lysines towards the substrate and the PEG chains projecting away from the surface.[169]

For the dithiol supported nanopatterns developed in the thesis works, PEG with the molecular weight 5000 g/mol conjugated to a terminal maleimide was used to covalently link PEG to free sulfhydryls on the dithiol SAM. This PEG was used since it efficiently excluded binding of proteins from areas surrounding the gold nanoparticles, but allowed access to the nanoparticle surfaces when 10 nm nanoparticles were used. This was verified indirectly by measuring the amount of protein that could bind to surfaces with different amount of particles.

The location of PEG molecules at areas surrounding the nanoparticles was further verified by AFM (Appendix B), indicating an apparent height of two to three nanometers for PEG in the dry state. Upon hydration, the molecule will require more space. Most clearly, the effect of PEG grafting can be seen in the phase pictures, which reflects the material properties rather than geometry. Upon modification with PEG, a phase shift can be seen for all areas except for the peak of each particle. Note that as always for AFM, the obtained pictures represent both the appearance of the surface and the AFM tip. Since particles were smaller than the tip, the lateral extensions of the nanoparticles appear too large.

This modification was introduced in **paper III** where it was used to prepare nanopatterns with a controlled amount of different polymers loaded onto the nanoparticles. These patterns were then used for cell studies in order to determine any dose-response effect between number of exposed polymers and the number and size of adhered cells. In **paper IV**, the same modification was applied on a nanoparticle gradient pattern as described in chapter 6. In addition, nanoparticle gradients were prepared where thiolated PEG (MW 5000 g/mol) was bound on top of distributed particles.

For the two types of gradient surfaces, the area available for site-specific protein modifications was then defined by the particle surface or the area between the particles respectively. Since the thiol-grafted PEG molecules were protruding a few nanometers from the particle surfaces, the area between particles are fully blocked as particles eventually come closer in the high coverage end of the gradient surface. Thus, whereas the first surface constitutes a gradient in number density of binding points, the second version is a gradient in domain size.

7.2.5 Characterization of site-specific modifications

A delicate matter regarding site-specific modifications of nanscopic features on surfaces is how such modifications can be characterized. Ultimately, both the identity, number of molecules, location and status of the bound molecules should be determined. Such measurements are hampered by the smallness of the nanostructures; some nanosized features may only bind one or very few molecules. In addition, if modified domains are widely separated on the substrate, the effective surface coverage will be low, and even their collective signal on the surface will be difficult to determine.

One technique with excellent resolution is AFM, which can be used to probe site-specific modifications on spot. AFM primarily measures changes in topography and material properties, and is frequently used to visualize proteins bound to surfaces.[170] The technique is adaptable to different circumstances and can deliver in-depth data, however the analysis can also be complicated, sometimes unambiguous and acquisition of data is intricate.

Techniques based on fluorescent labeling, e.g. fluorescence microscopy, and mass spectroscopic methods, e.g. time-of-flight secondary ion mass spectroscopy (TOF-SIMS) are useful since they allow the identification of bound species. Usually, these techniques have a low limit of detection; however, measurements are not quantitative, at least not without an internal reference. With ordinary fluorescence microscopy, individual spots on a surface cannot be visualized unless they are separated a few hundred nanometers from each other.

Techniques suitable for quantification of the number of bound molecules are among others QCM-D (Quartz Crystal Microbalance with Dissipation monitoring)[171], SPR and ellipsometry[46]. These techniques can be used to measure the accumulated mass of adsorbed species, with the distinction that QCM-D measures the mass of molecules included associated water[172], whereas the optical techniques measures the dry mass. Thus, optical techniques are best suited for determination of number of bound molecules, which can be obtained by scaling the optical mass with the molecular weight.

For the mentioned systems, data on mass adsorption represents an average obtained from a specified area, commonly in the mm^2 range. Thus, the number

of molecules binding to a nanoscopic feature can be estimated from the amount of molecules bound to a homogenous surface with similar chemical properties by geometric scaling.

This approach is straightforward, but can also be problematic; nanosized features usually have more curvature compared to extended substrates, which can influence adsorption behavior. For lithographically engineered nanopatterns involving the use of resists and sacrificial layers, there can also be a discrepancy in cleanliness between homogenous surfaces and patterned. Optimally, mass adsorption experiments should therefore be done on intact nanopatterns fabricated on sensor surfaces. For most patterns, this can be done with QCM-D, since the quartz crystals used as substrate can be coated with thin films of suitable substrate material, e.g. gold or silicon dioxide without interfering with the measurements dynamics[173].

With SPR, this is less straightforward since thin gold films coated on glass are the required substrates and the sensitivity is limited to the area closest to the gold film. However, since gold substrates were used for the preparation of dithiol-supported nanopatterns, these could also be prepared on top of commercial SPR substrates. This was used in **paper II** in order to characterize the number of bound polymer molecules on top of each nanoparticles as well as the subsequent binding of growth factors to the nanoparticle-polymer assemblies.

In **paper IV**, this approach was further extended when a system for imaging SPR (iSPR)[174] located at Linköping University was used for spatially resolved measurements on nanoparticle gradients. Since the 10 nm gold nanoparticles themselves gave a large response, iSPR was used both to characterize the particle gradients and the subsequent binding of proteins to these surfaces, thereby allowing a straightforward correlation between the particle density and

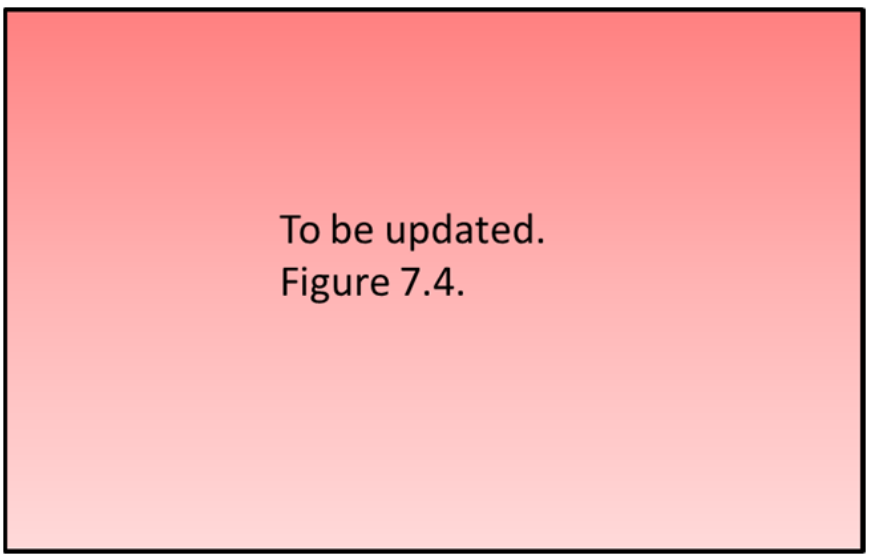

amount of bound protein (figure 7.4).

It should be noted that the introduction of metallic, plasmon active particles on a SPR sensor should be treated with some concern. However, the particles are separated from the gold substrate by the dithiol monolayer and are therefore not considered as a part of the underlying gold. To some extent, coupling between surface plasmons and the localized nanoparticle plasmons will occur. These effects are however size-dependent and will be small for particles ≤10 nm in diameter when the surface plasmon is excited at wavelengths far away from the nanoparticle plasmon resonance[175,176].

For the 10 nm nanoparticles used in these studies, it is likely that the SPR shift mainly correlates to the particles' accumulated mass, rather than their electronic properties.[177] Correlation between iSPR data and SEM micrographs revealed a linear relation between the particle density and the SPR response.

8. Summary of papers

Paper I

Self-arrangement among charge-stabilized gold nanoparticles on a dithiothreitol reactivated octanedithiol monolayer

A. Lundgren, F. Björefors, L. Olofsson, H. Elwing

Nano Letters (8) 2008, 3989-3992

Contribution
I planned the work and performed all experiments except for the scanning electron microscopy. I also evaluated the results and wrote the manuscript.

Description and comments
This work was initiated within the EU-funded industrial research project NACARDIO, with the aim to develop an electrical biosensor technique based on electron tunneling between solid gold electrodes and supported gold nanoparticles. Considerable work was devoted to the realization of a surface modification that allowed effective particle immobilization. The octanedithiol were a suitable candidate since it formed isolating, but not too thick monolayers, important for electron tunneling to occur.

The preparatory work involved many electrochemical evaluations, some of them discussed in chapter 2 in this thesis. With the aim to maximize the number of bound particles, a systematic study of factors influencing the particle binding was undertaken, which revealed a strong dependence on electrolyte concentrations as discussed in chapter 5.

In short: It was shown that gold nanoparticles self-assembled onto a homogeneous dithiol monolayer could arrange in a controllable fashion due to particle electrostatic interactions and that interparticle distance could be predicted by DLVO theory. Local tendencies toward long-range ordering could be seen among the bound particles, which possibly were related to the particles'

small size but also due to the superior homogeneity and reactivity of the surface modification.

A direct comparison was done between octanedithiol modified gold and silicon wafers modified with (3-mecaptopropyl)trimethoxysilane showing that silane-coated surfaces had a lower binding capacity when immersed in the same particle solution. Initial experiments with chemical grafting of maleimide-conjugated poly(ethylene glycol) to the nanoparticle modified surfaces were performed. These experiments are presented in the supporting info appended to the article.

Paper II

Immune complement activation is attenuated by surface nanotopography

M. Hulander, A. Lundgren, M. Berglin, M. Ohrlander, J. Lausmaa, H. Elwing

International Journal of Nanomedicine (11) 2011, 2653–2666

Contribution

This was mainly the work of MH. I contributed to the development of the surface preparation protocol, the planning of some experiments, analysis of results and to some extent with the writing of the manuscript.

Description and comments

The immune complement (IC) is a cell-free protein cascade system, and the first part of the innate immune system to recognize foreign objects entering the body. Elevated activation of the system from, for example, biomaterials or medical devices can result in both local and systemic adverse effects and eventually loss of function or rejection of the biomaterial.

Surface activation of the immune complement has been in focus in a range of papers from prof. Elwing's laboratory, however this was the first study specifically devoted to nanostructured surfaces. Based on earlier experiments made on commercial biomaterial coatings, we hypothesized that 50 nm gold nanoparticles adsorbed to and sintered into a surface would affect the surface activation of the innate immune response. Gold surfaces treated this way were shown to display a nanostructured but chemically homogenous surface, as determined with XPS (X-ray Photoelectron Spectroscopy) and TOF-SIMS.

In short: The activation of the IC on smooth and nanostructured surfaces incubated in human serum was studied with fluorescence microscopy and quantified with quartz crystal microbalance with dissipation monitoring using antibodies binding to complement factor C3. Additionally, the ability of pre-adsorbed human immunoglobulin G (IgG), a potent activator of the immune complement, to activate the IC after a change in surface hydrophobicity was studied. It was found that the activation of the IC was significantly attenuated on nanostructured surfaces with nearly a 50% reduction, even after pre-adsorption with IgG. An increase in surface hydrophobicity blunted this effect.

Possible mechanisms for this, somewhat unexpected, result were discussed and we suggested that the curvature of the nanoparticles could be an important factor. The curvature of the surface supported nanostructures may influence the orientation of the adsorbed IgG molecules, hampering the interactions between IgG and complement factor C1q. This mechanism was supported by investigations made by others on the protein corona of polymeric nanoparticles incubated in plasma, where C1q were absent on hydrophilic but present on hydrophobic particles with the same size as in our work.

Paper III

Self-Assembled Arrays of Dendrimer-Gold Nanoparticle Hybrids for Functional Cell Studies

A. Lundgren, Y. Hed, K. Öberg, A. Sellborn, H. Fink, P. Löwenhielm, J. Kelly, M. Malkoch, M. Berglin

Angew. Chem. Int. Ed. 2011, 50, 3450 –3453

Contribution

I took part in the planning of the work, performed most surface preparations, SPR experiments and SEM analysis. I also contributed significantly to the analysis of the results and wrote the manuscript draft.

Description and comments

This project was a collaboration between our lab, School of Chemistry and Chemical Science at the Royal Institute of Technology and Mölnlycke Health Care AB, with the aim to investigate the usefulness of some novel polymeric materials - dendrimers - in wound-healing applications. Dendrimers are highly branched, spherical-shaped polymers with an inherently high end-group concentration. It was hypothesized that these properties would increase the availability and multivalency of cell-interacting ligands with dendrimers compared to linear polymers with similar chemical composition. We therefore wanted to examine the cell viability on surfaces with a controlled amount of respective ligand presented on an otherwise inert background.

In short: Arrays of distributed gold nanoparticles were prepared as outlined in **paper I**. These were modified with maleimide-conjugated PEG between distributed particles and the particle surfaces were modified with a novel carboxylated dendrimer and polyacrylic acid respectively. The negatively charged polymers were electrostatically bound to the particles, which were made positively charged by reaction with mercaptoetanolamine. The chemical modifications were verified using ToF-SIMS, QCM-D and SPR. From SPR-data, we calculated an approximately one to one relation between particles and polymers.

The number and morphology of primary human endothelial cells grown on these surfaces was studied, and it was seen that the dendrimer-coated nanoparticle arrays potentiated cell-growth to a larger extent than nanoparticle arrays coated with the linear counterpart. As a possible mechanism, we discussed the possibility that the dendrimers, due to their spherical shape and highly charged surface, may adsorb a larger amount of cell-stimulating proteins from the cell media. Using SPR, we observed a larger binding of the endothelial cell growth factor (ECGF) onto nanoparticle arrays coated with the carboxylated dendrimer compared to the linear polyacrylic acid.

Paper IV

Tuning molecular compartmentalization via nanoparticle self-assembly, implications for classical cell adhesion experiments

A. Lundgren, M. Hulander, M. Hermansson, H. Elwing, O. Andersson,
B. Liedberg, P. Sjöwall, M. Berglin

In manuscript

Contribution

I planned most of the work together with MB. I designed the gradient fabrication technique, did all modeling and most surface preparations. I also took part in iSPR, TOF-SIMS, SEM and CLSM analysis as well as the evaluation of the results. I wrote the manuscript draft.

Description and comments

This paper summarizes important developments of the nanoparticle patterning approach done after **paper III**. The main novelties are the introduction of a nanoparticle gradient surface and an "inverse" type of surface modification, where the nanoparticles were modified with PEG and areas surrounding the particles were made adhesive or functionalized with proteins.

The idea of a gradient surface came up during the work with the polymer-modified nanoparticle arrays. Since the size and morphology among cells in a population grown on a surface can be rather heterogeneous, we assumed that a gradient would facilitate the analysis of both linear behavior and cut-off phenomena. The basic gradient fabrication approach is an extension of Prof. Elwing's set-up for fabrication of wettability gradients with the important difference that here we did not diffuse the reactant itself, but the ions *controlling* the deposition of the reactant.

The first aim of this paper was to demonstrate that nanoparticle assembly combined with site-specific molecular grafting is a powerful and versatile tool for nanoscopic control of the molecular compartmentalization on a surface. Secondly, we wanted to demonstrate the usefulness of the gradient surfaces for the detection of complex binding phenomena. As proof-of-concept, we performed "classical" cell adhesion experiments; bacterial adhesion to hydrophobic nanodomains as well as the adhesion and morphological

development of primary fibroblasts to protein and peptide modified surfaces was investigated.

In short: The procedure for fabrication of nanoparticle gradients on dithiol modified gold surfaces via ion diffusion was described and modeled. The nanoparticle gradient surfaces were chemically modified with PEG-maleimides between the distributed particles whereas the particle surfaces were modified to become cell-binding using thiolate chemistry. Alternatively, the particle surfaces were modified with PEG-thiols whereas surrounding areas were made adhesive using maleimide chemistry. The following strategies to modify adhesive domains were demonstrated:

(i) site-specific grafting of non-polar methylated molecules, i.e octanethiol and methylmaleimide to particle surfaces and surrounding areas respectively.
(ii) adsorption of proteins to hydrophobic domains.
(iii) modification of areas between the particles with biotin-maleimide, allowing the subsequent modification with streptavidin and other biotinylated proteins or peptides.
(iv) binding of functional thiols, conjugated to peptides and other functional groups to the nanoparticle surfaces.

In a first experiment, the unspecific adhesion of fimbriae-carrying *E. coli* was investigated on gradients with hydrophobic compartments. Hydrophobic modifications on top of and between distributed particles were verified by water contact angle measurements at all positions of the gradient surfaces using the Wilhelmy plate technique. We found that the bacterial binding was largely dependent on the size of the adhesive domain. For small domains, ~10 nm in diameter, bacteria bound in direct relation to the number of domains, forming stable bonds. For larger hydrophobic domains bacteria bound in large number, but most of these bacteria were loosely bound. For very small domains, no binding was seen.

The different binding could not be predicted by the water contact angle measurements, which gave similar values irrespective of the molecular compartmentalization. We suggested that bacterial binding to smaller domains primarily was mediated via fimbriae. The availability of the small domains to

fimbriae was verified using gradient surfaces where particles were modified with thiolated mannose, which bind specifically to the *E. coli* fimbria.

In a second experiment, the adhesion and morphological development of normal human dermal fibroblasts (NHDF) to gradient surfaces modified with RGD-peptides or one of the two proteins fibrinogen or fibronectin, both having the RGD motif, was investigated. Gradients were modified with PEG on top of the particles and proteins/peptides were bound to the domains between distributed particles. Gradient surfaces were also prepared with RGD peptides, where PEG was replaced with heparin on the particle surfaces.

Protein modifications were characterized by imaging SPR. Modifications with peptides were verified with TOF-SIMS as well as the distribution of PEG and heparin respectively. These characterizations showed that gradients modified with PEG and proteins/peptides had a smooth appearance ranging from zero protein binding at the high PEG end to approximately 0.75 monolayer coverage at the low PEG end. For gradients modified with heparin, zero binding was not reached at the high heparin end, resulting in a weaker RGD gradient.

Cells grown on the gradient coated with fibronectin and PEG were all well spread, also on the part with very low protein coverage. Only a weak dependence could be seen between the fibronectin coverage and the number of cells. In contrast, the gradient modified with RGD peptide, showed a strong dependence between RGD coverage and both the number of cells and the size of the cells. Cells positioned at the end with low RGD coverage were all round, whereas some cells in the central part of the gradient were elongated and appeared to be migrating. Cells positioned at the end with high RGD were flattened, but less developed than for fibronectin.

The gradient modified with fibrinogen and PEG appeared similar to the gradient modified with RGD and PEG, displaying the same types of cell morphologies at the same position. However, in comparison more migrating cells were seen in the central part of the fibrinogen gradient compared to the RGD counterpart. The most complex behavior was seen for gradients with RGD peptides where PEG was replaced with heparin. As observed for gradients modified with RGD-PEG, an increase in RGD promoted the cell adhesion giving a larger number of cells. However, a reversed correlation was also seen where increased coverage

of heparin promoted cell polarization. The results correlating to cell migration was discussed in the context of wound healing.

9. Concluding remarks and outlook

In conclusion,

I have shown that small, charged nanoparticles can be made to self-organize on a binding substrate under the influence of electrostatic double-layer forces. The particle interactions on the surfaces could be described within the framework of classical DLVO-theory, and the separation of gold nanoparticles 5-30 nm in diameter could readily be tuned by the ionic composition of the particle solution. A novel method to prepare surfaces with nanoparticle gradients, based on ion diffusion, was introduced. These surfaces were used as versatile templates for the preparation of nanopatterns of chemical entities and proteins, with a periodicity in the sub 100 nm regime, eventually reaching single-molecule resolution. The applicability of these patterns for research related to interface biology was demonstrated.

For future work, the introduction of particles with other geometry than spherical, or a different composition, would add new possibilities to form different functional nanocompartments on substrates. The use of such patterns is not limited to biological applications, but could be useful within different areas of material science. In addition, the gradient approach can be extended; work in progress aims at the assembly of gradients with higher dimensionality by the use of ion diffusion in three dimensions.

Patterning of non-flat substrates, e.g. microfibers, is of interest for use in three-dimensional cell models. Possibly, microfluidics could also be used to control ion composition and thereby create patterns not possible to prepare with ion diffusion. Furthermore, using bi-polar electrochemistry, we recently demonstrated that gold (or other metal) could be site-specifically deposited onto already bound particles in a potential dependent manner, thereby forming gradients in particle size on a surface. Thus, the self-organization approach has considerable potential to form the basis for a long range of functional surface coatings or patterns with extraordinary resolution.

From a biological point of view, the work described in this thesis had a broad focus in terms of subjects. Thus, in relation to the wealth of literature and studies devoted to these issues, the contribution of my works should not be exaggerated. However, I want to point out a few findings with relevance for future work:

The deposition of proteins related to acute phase immune response was seen to be attenuated by the incorporation of nanostructure on a surface. Considering the interconnections between the early immune response and immunization, mediated by immune cells, these findings may be important for an increased understanding of these processes and thereto-related applications such as vaccine development. In addition, other protein cascade systems, e.g. blood coagulation, may show similar responsiveness for nanostructured surfaces. Thus, the interface between nanostructures and proteins is an area that needs further consideration, not at least for a better understanding of secondary cell-interactions.

The binding of fimbriated *E. coli* bacteria was found to be very dependent on the organization of adhesive and non-binding molecules on surfaces. These effects could not be predicted from measurements of water contact angle, but required control of the nanoscopic molecular arrangements in the sub 100 nm regime. The analysis of this non-linear binding phenomenon was significantly facilitated by the use of gradient surfaces displaying a continuously changing surface composition. Thus, gradient surfaces in general are well suited for studies on adhesion mechanisms and surface-controlled cell functionality.

Another finding with relation to gradient surfaces was the high polarization and alignment among the cells, which was observed for some modifications. This implies a high degree of directed cell migration, which should be verified with live-cell imaging studies. The study of cell migration is of great interest, not at least in the context of cancer metastasis and wound healing. Gradient surfaces may provide a good model system for studies within these areas. Of special interest is protein remodeling in relation to cell migration, which would be interesting to study in live cells experiments using imaging SPR.

References

1 Lodish, H. *et al. Molecular cell biology*. 4 edn, (W. H. Freeman and Company, 1999).

2 Mecham, R. P. *The Extracellular Matrix: an Overview*. (Springer-Verlag, 2011).

3 Capila, I. & Linhardt, R. J. Heparin-Protein Interactions. *Angewandte Chemie International Edition* **41**, 390-412 (2002).

4 Ruhrberg, C. *et al.* Spatially restricted patterning cues provided by heparin-binding VEGF-A control blood vessel branching morphogenesis. *Genes & Development* **16**, 2684-2698 (2002).

5 Place, E. S., Evans, N. D. & Stevens, M. M. Complecity in biomaterials for tissue engineering. *Nature Materials* **8**, 457-470 (2009).

6 Reubinoff, B. E., Pera, M. F., Fong, C. Y., Trounson, A. & Bongnso, A. Embryonic stem cell lines from human blastocysts: somatic differentiation in vitro. *Nature Biotechnology* **18**, 399-404 (2000).

7 McMurray, R. J. *et al.* Nanoscale surfaces fo the long-term maintenance of mesenchymal stem cell phenotype and multipotency. *Nature Materials* **10**, 637-644 (2011).

8 Geiger, B., Spatz, J. P. & Bershadsky, A. D. Environmental sensing through focal adhesions. *Nature Reviews Molecular Cell Biology* **10**, 21-33 (2009).

9 Whitesides, G. M., Mathias, J. P. & Seto, C. T. Molecular Self-Assembly and Nanochemistry: A Chemical Strategy for the Synthesis of Nanostructures. *Science* **254**, 1312-1319 (1991).

10 Daniel, M. & Asruc, D. Gold nanoparticles: Assembly, Supramolecular chemistry, Quantum-size-related Properties and Applications towards Biology, Catalysis and Nanotechnology. *Chemical Reviews* **104**, 293-346 (2004).

11 Verwey, E. J. W. & Overbeek, J. T. G. *Theory of the stability of lyophobic colloids*. (Elsevier Publishing Company Inc., 1948).

12 Derjaguin, B. V. & Landau, L. *Acta Physicochim.* **14**, 633 (1941).

13 M., W. G. & Grzybowski, B. Self-assemblt at all scales. *Science* **295**, 2418-2421 (2002).

14 Lehn, J.-M. Toward complex matter: Supramolecular chemistry and self-organization. *Proc. Natl. Acad. Sci. U. S. A.* **99**, 4763-4768 (2002).

15 Rothemund, P. W. K. Folding DNA to create nanoscale shapes and patterns. *Nature* **440**, 297-302 (2006).

16 Mirkin, C. A., Letsinger, R. L., Mucic, R. S. & Storhoff, J. J. A DNA-based method for rationally assembling nanoparticles into macroscopic materials. *Nature* **382**, 607-609 (1996).

17 Alvisatos, A. P. *et al.* Organizaton of "nanocrystal molecules" using DNA. *Nature* **382**, 609-611 (1996).

18 Aili, D. *et al.* Folding Induced Assembly of Polypeptide Decorated Gold Nanoparticles. *J. Am. Chem. Soc.* **130**, 5780-5788 (2007).

19 Hartgerink, J. D., Beniash, E. & Stupp, S. I. Peptide-amphiphile nanofibers: A versatile scaffold for the preparation of self-assembling materials. *Proc. Natl. Acad. Sci. U. S. A.* **99**, 5133-5138, doi:10.1073/pnas.072699999 (2002).

20 Niece, K. L., Hartgerink, J. D., Donners, J. & Stupp, S. I. Self-assembly combining two bioactive peptide-amphiphile molecules into nanofibers by electrostatic attraction. *J. Am. Chem. Soc.* **125**, 7146-7147, doi:10.1021/je028215r (2003).

21 Tysseling-Mattiace, V. M. *et al.* Self-assembling nanofibers inhibit glial scar formation and promote axon elongation after spinal cord injury. *J. Neurosci.* **28**, 3814-3823, doi:10.1523/jneurosci.0143-08.2008 (2008).

22 Ulman, A. Formation and structure of self-assembled monolayers. *Chemical Reviews* **96**, 1533-1554 (1996).

23 Vanderberg, E. *et al.* Structure of 3-aminopropyl triethoxy silane on silicon-oxide. *Journal of Colloid and Interface Science* **147**, 103-118 (1991).

24 Keller, C. A. & Kasemo, B. Surface specific kinetics of lipid vesicle adsorption measured with a quartz crystal microbalance. *Biophysical Journal* **75**, 1397-1402 (1998).

25 Reimhult, E., Höök, F. & Kasemo, B. Intact Vesicle Adsorption and Supported Biomembrane Formation from Vesicles in Solution: Influence of Surface Chemistry, Vesicle Size, Temperature, and Osmotic Pressure. *Langmuir* **19**, 1681-1691 (2003).

26 Nuzzo, R. G. & Allara, D. L. Adsorption of Bifunctional organic disulfides on gold surfaces. *J. Am. Chem. Soc.* **105**, 4481-4483 (1983).

27 Love, J. C., estroff, L. A., Kriebel, J. K. N., R. G. & Whitesides, G. M. Self-Assembled Monolayers of Thiolates on Metals as a Form of Nanotechnology. *Chemical Reviews* **105**, 1103-1169 (2005).

28 Porter, M. D., Bright, T. B., Allara, D. L. & Chidsey, C. E. D. Spontaneously Organized Molecular Assemblies .4. Structural Characterization of Normal-Alkyl Thiol Monolayers on Gold by Optical Ellipsometry, Infrared-Spectroscopy, and Electrochemistry. *J. Am. Chem. Soc.* **109**, 3559-3568 (1987).

29 Prime, K. L. & Whitesides, G. M. Self-Assembled Organic Monolayers - Model Systems for Studying Adsorption of Proteins at Surfaces. *Science* **252**, 1164-1167 (1991).

30 Tengvall, P., Lundström, I. & Liedberg, B. Protein adsorption studies on model organic surfaces: an ellipsometric and infrared spectroscopic approach. *Biomaterials* **19**, 407-422 (1998).

31 Lofas, S. *et al.* Bioanalysis with Surface-Plasmon Resonance. *Sensors and Actuators B-Chemical* **5**, 79 (1991).

32 Flink, van Veggel, F. C. J. M. & Reinhouldt, D. N. Sensor Functionalities in Self-Assembled Monolayers. *Advanced Materials* **12**, 1315-1328 (2000).

33 Shipway, A. N., Lahav, M. & Willner, I. Nanostructured Gold Colloid Electrodes. *Advanced Materials* **12**, 993-998 (2000).

34 Dubois, L. H. & Nuzzo, R. G. Synthesis, Structure, and Properties of Model Organic-Surfaces. *Annual Review of Physical Chemistry* **43**, 437-463 (1992).

35 Liedberg, B. & Cooper, J. M. in *Immobilized Biomolecules in Analysis: A Practical Approach* (Oxford university press, 1998).

36 Wirde, Gelius, U. & Nyholm, L. Self-Assembled Monolayers of Cystamine and Cysteamine on Gold studied by XPS and Voltammetry. *Langmuir* **15**, 6370-6378 (1999).

37 Uvdal, K., Bodö, P. & Liedberg, B. L-Cysteine Adsorbed on Gold and Copper; An X-ray Photoelectron Spectroscopic Study. *Journal of Colloid and Interface Science* **149**, 162-173 (1992).

38 Hermansson, G. T. *Immobilized affinity ligands techniques*. (Academic Press Inc., 1992).

39 Freeman, R. G. *et al.* Self-Assembled Metal Colloid Monolayers: An approach to SERS Substrates. *Science* **267**, 1629-1632 (1995).

40 Grabar, K. C. *et al.* Kinetic control of interparticle spacing in Au colloid-based surfaces: Rational nanometer-Scale Architecture. *J. Am. Chem. Soc.* **118**, 1148-1153 (1996).

41 Carot, M. L., Esplandiu, M. J., Cometto, F. P., Patrito, E. M. & Macagno, V. A. Reactivity of 1,8-octanedithiol monolayers on Au(111): Experimental and theoretical investigation. *Journal of Electroanalytical Chemistry* **579**, 13-23 (2005).

42 Esplandiu, M. J., Carot, M. L., Cometto, F. P., Macagno, V. A. & Patrito, E. M. Electrochemical STM investigation of 1,8-octanedithiol monolayers on Au(111). Experimental and theoretical study. *Surface Science* **600**, 155-172 (2006).

43 Rieley, H., Kendall, G. K., Zemicael, F. W., Smith, T. L. & Yang, S. X-ray studies of self-assembled monolayers on coinage metals. 1. Alignment and Photooxidation in 1,8-octanedithiol and 1-octanethiol on Au. *Langmuir* **14**, 5147-5153 (1998).

44 Aliganga, A. K. A., Duwez, A.-S. & Mittler, S. Binary mixtures of self-assembled monolayers of 1,8-octanedithiol for a controlled growth of gold nanoparticles. *Organic Electronics* **7**, 337-350 (2006).

45 Cleland, W. W. Dithiolthreitol, a new protective reagent for SH groups. *Biochemistry* **3**, 480-482 (1964).

46 Arwin, H. Ellipsometry on thin organic layers of biological interest: characterization and applications. *Thin Solid Films* **377**, 48-56 (2000).

47 Bard, A. J. & Faulkner, L. R. *Electrochemical Methods*. 2:nd edn, (John Wiley & Sons Inc., 2001).

48 Widrig, C. A., Chung, C. & Porter, M. D. The electrochemical desorption of n-alkanethiol from polycrystalline Au and Ag electrodes. *Journal of Electroanalytical Chemistry* **310**, 335-359 (1991).

49 Yang, D.-F., Wilde, C. P. & Morin, M. Electrochemical Desorption and Adsorption of Nonyl Mercaptan at Gold Single Crystal Electrode Surfaces. *Langmuir* **12**, 6570-6577 (1996).

50 Hobara, D., Miyake, O., Imabayashi, S., Niki, K. & Kakiuchi, T. Phase separation of binary self-assembled thiol monolayers composed of 1-hexadecanethiol and 3-mercaptopropionic acid on Au(111) studied by scanning tunneling microscopy and cyclic valtammetry. *Journal of Electroanalytical Chemistry* **444**, 113-119 (1998).

51 Wong, S. & Porter, M. D. Origin of the multiple voltammetric desorption waves of long-chain alkanethiolate monolayers chemisorbed on annealed gold electrodes. *Journal of Electroanalytical Chemistry* **485**, 135-143 (2000).

52 Zhong, C.-J. & Porter, M. D. Fine structure in the voltammetric desorption curves of alkanethiolate monolayers cherr sorbed at gold. *Journal of Electroanalytical Chemistry* **425** (1997).

53 Kohli, P., Taylor, K. K., Harris, J. J. & Blanchard, G. J. Assembly of covalently-coupled disulfide multilayers on gold. *J. Am. Chem. Soc.* **120**, 11962-11968 (1998).

54 Ohgi, T., Sheng, H.-Y., Nejoh, H., Dong, Z.-C. & D., F. Charging effects in gold nanoclusters grown on octanedithiol layers. *Applied Physics Letters* **79**, 2453-2455 (2001).

55 Faraday, M. Experimental relations of gold (and other metals) to light. *Philos. Trans.* **147**, 145-181 (1857).

56 Turkevich, K., Stevenson, P. J. & Hillier, J. Nucleation and Growth Process in the Synthesis of Colloidal Gold. *Discussions of the Faraday Society* **11**, 55-75 (1951).

57 Frens, G. Controlled Nucleation for the Regulation of the Particle Size in Monodisperse Gold Suspensions. *Nature Physical Science* **241**, 20-22 (1973).

58 Brust, M., Wlaker, M., Bethell, D., Schiffrin, D. J. & Whyman, R. Synthesis of Thiol-Derivatized Gold Nanoparticles in a 2-PhaseLiquid-Liquid System. *Journal of Chemical Society, Chemical Communications* **7**, 801-802 (1994).

59 Mülpfordt, H. The preparation of colloidal gold particles using tannic acid as an additional reducing agent. *Experientia* **38**, 1127-1128 (1982).

60 Faulk, W. & Taylor, G. An immunocolloid method for the electron microscope. *Immunochemistry* **8**, 1081-1083. (1971).

61 Slot, W. J. & Geuze, H. J. Sizing of Protein A-colloidal probes for immunoelectronmicroscopy. *Journal of Cell Biology* **90** (1981).

62 Shipway, N. A., Katz, E. & Willner, I. Nanoparticle Arrays on Surfaces for Electronic, Optical, and Sensor Applications *CHEMPHYSCHEM* **1**, 18-52 (2000).

63 Chen, S. W. *et al.* Gold nanoelectrodes of varied size: Transition to molecule-like charging. *Science* **280**, 2098-2101 (1998).

64 Storhoff, J. J. *et al.* What Controls the Optical Properties of DNA-Linked Gold Nanoparticle Assemblies? *J. Am. Chem. Soc.* **122**, 4640-4650 (2000).

65 Frederix, F. *et al.* Biosensing Based on Light Absorption of Nanoscaled Gold and Silver Particles. *Analytical Chemistry* **75**, 6894–6900 (2003).

66 Raj, C. R., Okajima, T. & Ohsaka, T. Goldnanoparticlearrays for the voltammetricsensing of dopamine. *Journal of Electroanalytical Chemistry* **543**, 127-133 (2003).

67 Nath, N. & Chilkoti, A. A Colorimetric Gold Nanoparticle Sensor To Interrogate Biomolecular Interactions in Real Time on a Surface. *Analytical Chemistry* **74**, 504-509 (2002).

68 Hostetler, M. J. *et al.* Alkanethiolate gold cluster molecules with core diameters from 1.5 to 5.2nm; monolayer properties as a function of core size. *Langmuir* **14**, 17-30 (1998).

69 Zheng, M. & Huang, X. Y. Nanoparticles comprising a mixed monolayer for specific bindings with biomolecules. *J. Am. Chem. Soc.* **126**, 12047-12054 (2003).

70 Mie, G. Beiträge zur Optik trüber Medien, speziell kolloidaler Metallösungen. *Annalen det Physic* **25**, 377-445 (1908).

71 Link, S. & El-Sayed, M. A. Size and temperature dependence of the plasmon resonence absoption of colloidal gold nanoparticles. *Journal of Physical Chemistry B* **103**, 4212-4217 (1999).

72 Himmelhaus, M. & Takei, H. Cap-shapedgoldnanoparticles for an opticalbiosensor. *Sensors and Actuators B* **63**, 24-30 (2000).

73 Oloffson, L., Rindzevicius, T., Pfeiffer, I., Käll, M. & Höök, F. Surface-based gold-nanoparticle sensor for specific and quantitative DNA hybridization detection. *Langmuir* **19**, 10414-10419 (2003).

74 Su, K. *et al.* Interparticle Effects on Nanogold Particles. *Nano Letters* **3**, 1087-1090 (2003).

75 Israelachvili, J. N. *Intermolecular and surface forces*. (Academic Press, 1992).

76 Kunze, J., Burgess, I., Nichols, R., Buess-Herman, C. & Lipkowski, J. Electrochemical evaluation of citrate adsorption on Au(111) and the stability of citrate-reduced gold colloids. *Journal of Electroanalytical Chemistry* **599**, 147-159 (2007).

77 Ohshima, H., Healy, T. W. & White, L. R. Accurate Analytic Expressions for the Surface Charge Density/Surface Potential Relationship and Double-Layer Potential Ditribution for a Spherical Colloidal Particle. *Journal of Colloid and Interface Science* **90**, 17-26 (1982).

78 Kim, T., Lee, K., Gong, M.-s. & Joo, S.-W. Control of Gold Nanoparticle Aggregates by Manipulation of Interparticle Interaction. *Langmuir* **21**, 9524-9528 (2005).

79 Cumberland, S. L. & Strouse, G. F. Analysis of the nature of oxyanion adsorption on gold nanomaterial surfaces. *Langmuir* **18**, 269-276, doi:10.1021/la011278n (2002).

80 Brewer, S. H., Glomm, W. R., Johnson, M. C., Knag, M. K. & Franzen, S. Probing BSA Binding to Citrate-Coated Gold Nanoparticles and Surfaces. *Langmuir* **21**, 9303-9307 (2005).

81 Sjollema, J. & Busscher, H. J. Deposition of Polystyrene Particles in a Parallel Plate Flow Cell. 2. Pair Distribution Functions Between Deposited Particles. *Colloids and Surfaces* **47**, 337-352 (1990).

82 Russel, W. B., Saville, D. A. & Schowalter, W. R. *Colloidal Dispersions*. (Cambridge University Press, 1989).

83 Kleimann, J. *et al.* Deposition of nanosized latex particles onto silica and cellulose surfaces studied by optical reflectometry. *Journal of Colloid and Interface Science* **303**, 460-471 (2006).

84 Adamczyk, Z., Zembala, M., Siwek, B. & Warszynski, P. Structure and ordering in localized adsorption of particles. *Journal of Colloid and Interface Science* **140** (1990).

85 Semmler, M., Ricka, J. & Borkovec, M. Diffusional deposition of colloidal particles: electrostatic interactions and size polydispersity effects. *Colloids and Surfaces A: Physicochemical and Engineering Aspects* **165**, 79-93 (2000).

86 Semmler, M., Mann, E. K., Ricka, J. & Borkovec, M. Diffusional deposition of charged latex particles on water-solid interfaces at low ionic strength. *Langmuir* **14**, 5127-5132 (1998).

87 Johnson, C. A. & Lenhoff, A. M. Adsorption of charged latex particles on Mica studied by atomic force microscopy. *Journal of Colloid and Interface Science* **179**, 587-599 (1996).

88 Hanarp, P., Sutherland, D. S., Gold, J. & Kasemo, B. Control of nanoparticle film structure for colloidal lithography. *Colloids and Surfaces A: Physicochemical and Engineering aspects* **214**, 23-36 (2003).

89 Guillame-Gentil, O. *et al.* Engineering the Extracellular Environment: Strategies for Building 2D and 3D Cellular Structures. *Advanced Materials* **22**, 5443-5462, doi:10.1002/adma.201001747 (2010).

90 Larsson, E., Langhammer, C., Zori, I. & Kasemo, B. Nanoplasmonic Probes of Catalytic Reactions. *Science* **326**, 1091-1094 (2009).

91 Agheli, H., Malmström, J., Hanarp, P. & Sutherland, D. S. Large Area Nanopatterning for Biological Applications. *Nano Letters* **6**, 1165-1171 (2006).

92 Michel, R. *et al.* A novel approach to produce biologically relevant chemical patterns at the nanometer scale: selective molecular assembly patterning combined with colloidal lithography. *Langmuir* **18**, 8580-8586 (2002).

93 Lin, X. M., Jaeger, H. M., Sorensen, C. M. & Klabunde, K. J. Formation of Long-Range-Ordered Nanocrystal Superlattices on Silicon Nitride Substrates. *Journal of Physical Chemistry B* **105**, 3353-3357 (2001).

94 Andres, R. P. *et al.* Self-Assembly of a Two-Dimensional Superlattice of Molecularly Linked Metal Clusters. *Science* **273**, 1690-1693 (1996).

95 Kiely, C. J., Fink, J., Brust, M., Bethell, B. & Shiffrin, D. J. Spontanous ordering of bimodal ensembles of nanoscopic gold clusters. *Nature* **396**, 444-446 (1998).

96 Förster, S. & Antonietti, M. Amphiphilic Block Copolymers in Structure-Controlled Nanometer Hybrids. *Advanced Materials* **10**, 195-217 (1998).

97 Spatz, J. P., Roescher, A. & Möller, M. Gold Nanoparticles in Micellar Poly(sryrene)-b-Poly(ethylene oxide) Films - Size and Interparticle Distance Control in Monoparticulate Films. *Advanced Materials* **8**, 337-340 (1996).

98 Spatz, J. P. *et al.* Ordered Deposition of inorganic Clusters from Micellar Block Copolymer Films. *Langmuir* **16**, 407-415 (2000).

99 Sohn, B.-H. *et al.* Directed Self-Assembly og Two Kinds of Nanoparticles Utilizing Monolayer Films of Diblock Copolymer Micelles. *J. Am. Chem. Soc.* **125**, 6368-6369 (2003).

100 Giersig, M. & Mulvaney, P. Preparation of Ordered Colloid Monolayers by Electrophoretic Deposition. *Langmuir* **9**, 3408-3413 (1993).

101 Bigioni, T. P. *et al.* Kinetically driven self assembly of highly ordered nanoparticle monolayers. *Nature* **5**, 265-270 (2006).

102 Brust, M. & Kiely, C. J. Some recent advances in nanostructure preparation from gold and silver particles: a short toppical review. *Colloids and Surfaces A: Physicochemical and Engineering Aspects* **202**, 175-196 (2002).

103 Leff, D. V., Brandt, L. & Heath, J. R. Synthesis and chracterization of hydrophobic organically-soluble gold nanocrystals functionalized with primary amines. *Langmuir* **12**, 4723-4730 (1996).

104 Ooka, A. A., Kuhar, K. A., Cho, N. J. & Garrell, R. L. Surface interactions of a homologous series of alpha,omega-amino acids on colloidal silver and gold. *Biospectroscopy* **5**, 9-17 (1999).

105 Bhat, R., Fischer, D. A. & Genzer, J. Fabricating Planar Nanoparticle Assemblies with Number Dansity Gradients. *Langmuir* **18**, 5640-5643 (2002).

106 Kooij, E. S., Brouwer, E. A. M., Wormeester, H. & Poelsema, B. Ionic strength mediated self-organisation of gold nanocrystals: an AFM study. *Langmuir* **18**, 7677-7682 (2002).

107 Langmuir, I. The adsorption of gases on plane surfaces of glass, mica and platinum. *J. Am. Chem. Soc.* **41**, 1361-1403 (1918).

108 Feder, J. Random Sequential Adsorption. *Journal of Theoretical Biology* **87**, 237-254 (1980).

109 Gray, J. J. & Bonnecaze, R. T. Adsorption of colloidal particles by Brownian dynamics simulation: Kinetics and surface structures. *Journal of Chemical Physics* **114**, 1366-1381 (2001).

110 Miyahara, M., Watanabe, S., Gotoh, Y. & Higashitani, K. Adsorption and order formation of colloidal nanoparticles on a substrate: A Brownian dynamics study. *Journal of Chemical Physics* **120**, 1524-1533 (2003).

111 Magan, R. & Sureshkumar, R. Multiscale-linking simulation of irreversible colloidal deposition in the presence of DLVO interactions. *Journal of Colloid and Interface Science* **297**, 389-406 (2006).

112 Brewer, D. D., Tsapatis, M. & Kumar, S. Dynamics of surface structure and evolution in colloidal adsorption: Charge patterning and polydispersity. *Journal of Chemical Physics* **133** (2010).

113 Wilson, C. J., Clegg, R. E., Leavesley, D. I. & Pearcy, M. J. Mediation of biomaterial-cell interactions by adsorbed proteins: A review. *Tissue Engineering* **11**, 1-18 (2005).

114 Bergkvist, M., Carlsson, J. & Oscarsson, S. Surface-dependent conformations of human plasma fibronectin adsorbed to silica, mica, and hydrophobic surfaces, studied with use of Atomic Force Microscopy. *J. Biomed. Mater. Res. Part A* **64A**, 349-356, doi:10.1002/jbm.a.10423 (2003).

115 Lehnert, M. *et al.* Adsorption and Conformation Behavior of Biotinylated Fibronectin on Streptavidin-Modified TiO(X) Surfaces Studied by SPR and AFM. *Langmuir* **27**, 7743-7751, doi:10.1021/la200908h (2011).

116 Globus, R. K. *et al.* Fibronectin is a survival factor for differentiated osteoblasts. *Journal of Cell Science* **111**, 1385-1393 (1998).

117 George, E. L., Georgeslabouesse, E. N., Patelking, R. S., Rayburn, H. & Hynes, R. O. DEFECTS IN MESODERM, NEURAL-TUBE AND VASCULAR DEVELOPMENT IN MOUSE EMBRYOS LACKING FIBRONECTIN. *Development* **119**, 1079-1091 (1993).

118 He, W. & Bellamkonda, R. V. Nanoscale neuro-integrative coatings for neural implants. *Biomaterials* **26**, 2983-2990, doi:10.1016/j.biomaterials.2004.08.021 (2005).

119 Rodin, S. *et al.* Long-term self-renewal of human pluripotent stem cells on human recombinant laminin-511. *Nature Biotechnology* **28**, 611-U102, doi:10.1038/nbt.1620 (2010).

120 Jensen, T. *et al.* Interaction of human mesenchymal stem cells with osteopontin coated hydroxyapatite surfaces. *Colloids and Surfaces B-Biointerfaces* **75**, 186-193, doi:10.1016/j.colsurfb.2009.08.029 (2010).

121 Martin, S. M., Schwartz, J. L., Giachelli, C. M. & Ratner, B. D. Enhancing the biological activity of immobilized osteopontin using a type-1 collagen affinity coating. *J. Biomed. Mater. Res. Part A* **70A**, 10-19, doi:10.1002/jbm.a.30052 (2004).

122 Shanmugasundaram, N. *et al.* Collagen-chitosan polymeric scaffolds for the in vitro culture of human epidermoid carcinoma cells. *Biomaterials* **22**, 1943-1951, doi:10.1016/s0142-9612(00)00220-9 (2001).

123 Ahmed, T. A. E., Dare, E. V. & Hincke, M. Fibrin: A versatile scaffold for tissue engineering applications. *Tissue Engineering Part B-Reviews* **14**, 199-215, doi:10.1089/ten.teb.2007.0435 (2008).

124 Cavalcanti-Adam, E. A., Aydin, D., Hirschfeld-Warneken, V. C. & Spatz, J. P. Cell adhesion and response to synthetic nanopatterned environments by steering receptor clustering and spatial location. *Hfsp Journal* **2**, 276-285, doi:10.2976/1.2976662 (2008).

125 Piner, R. D., Zhu, J., Xu, F., Hong, S. H. & Mirkin, C. A. "Dip-pen" nanolithography. *Science* **283**, 661-663, doi:10.1126/science.283.5402.661 (1999).

126 Slater, J. H. & Frey, W. Nanopatterning of fibronectin and the influence of integrin clustering on endothelial cell spreading and proliferation. *J. Biomed. Mater. Res. Part A* **87A**, 176-195, doi:10.1002/jbm.a.31725 (2008).

127 Malmstrom, J. *et al.* Focal Complex Maturation and Bridging on 200 nm Vitronectin but Not Fibronectin Patches Reveal Different Mechanisms of Focal Adhesion Formation. *Nano Letters* **11**, 2264-2271, doi:10.1021/nl200447q (2011).

128 Arnold, M. *et al.* Activation of integrin function by nanopatterned adhesive interfaces. *Chemphyschem* **5**, 383-388 (2004).

129 Lohmuller, T. *et al.* Supported Membranes Embedded with Fixed Arrays of Gold Nanoparticles. *Nano Letters* **11**, 4912-4918, doi:10.1021/nl202847t (2011).

130 Bellis, S. L. Advantages of RGD peptides for directing cell association with biomaterials. *Biomaterials* **32**, 4205-4210, doi:10.1016/j.biomaterials.2011.02.029 (2011).

131 Kammerer, P. W. *et al.* IMMOBILISATION OF LINEAR AND CYCLIC RGD-PEPTIDES ON TITANIUM SURFACES AND THEIR IMPACT ON ENDOTHELIAL CELL ADHESION AND PROLIFERATION. *European Cells & Materials* **21**, 364-372 (2011).

132 Fani, M. *et al.* Comparative evaluation of linear and cyclic Tc-99m-RGD peptides for targeting of integrins in tumor angiogenesis. *Anticancer Res.* **26**, 431-434 (2006).

133 Sawyer, A. A., Hennessy, K. M. & Bellis, S. L. The effect of adsorbed serum proteins, RGD and proteoglycan-binding peptides on the adhesion of mesenchymal stem cells to hydroxyapatite. *Biomaterials* **28**, 383-392, doi:10.1016/j.biomaterials.2006.08.031 (2007).

134 Benoit, D. S. W. & Anseth, K. S. The effect on osteoblast function of colocalized RGD and PHSRN epitopes on PEG surfaces. *Biomaterials* **26**, 5209-5220, doi:10.1016/j.biomaterials.2005.01.045 (2005).

135 Dalby, M. J. *et al.* Group analysis of regulation of fibroblast genome on low-adhesion nanostructures. *Biomaterials* **28**, 1761-1769 (2007).

136 Kilian, K. A., Bugarija, B., Lahn, B. T. & Mrksich, M. Geometric cues for directing the differentiation of mesenchymal stem cells. *Proc. Natl. Acad. Sci. U. S. A.* **107**, 4872-4877, doi:10.1073/pnas.0903269107 (2010).

137 Lundqvist, M., Sethson, I. & Jonsson, B. H. Protein adsorption onto silica nanoparticles: Conformational changes depend on the particles' curvature and the protein stability. *Langmuir* **20**, 10639-10647, doi:10.1021/la0484725 (2004).

138 Shang, W. *et al.* Cytochrome c on Silica Nanoparticles: Influence of Nanoparticle Size on Protein Structure, Stability, and Activity. *Small* **5**, 470-476, doi:10.1002/smll.200800995 (2009).

139 Roach, P., Farrar, D. & Perry, C. C. Surface tailoring for controlled protein adsorption: Effect of topography at the nanometer scale and chemistry. *J. Am. Chem. Soc.* **128**, 3939-3945, doi:10.1021/ja056278e (2006).

140 Wang, J. *et al.* Soft interactions at nanoparticles alter protein function and conformation in a size dependent manner. *Nano Letters* **11**, 4985-4991 (2011).

141 Lundqvist, M. *et al.* Nanoparticle size and surface properties determine the protein corona with possible implications for biological impacts. *Proc. Natl. Acad. Sci. U. S. A.* **105**, 14265-14270, doi:10.1073/pnas.0805135105 (2008).

142 Rodin, S. *et al.* Long-term self-renewal of human pluripotent stem cells on human recombinant laminin-511. *Nature Biotechnology* (2010).

143 Nakanishi, K., Sakiyama, T. & Imamura, K. On the adsorption of proteins on solid surfaces, a common but very complicated phenomenon. *J. Biosci. Bioeng.* **91**, 233-244, doi:10.1263/jbb.91.233 (2001).

144 Kleijn, M. & Norde, W. The adsorption of proteins from aqueous solution on solid surfaces. *Heterogeneous Chem. Rev.* **2**, 157-172 (1995).

145 Zubay, G. L. *Biochemistry*. 4:th edn, (The McGraw-Hill Companies, Inc., 1998).

146 Norde, W. & Giacomelli, C. E. BSA structural changes during homomolecular exchange between the adsorbed and the dissolved states. *Journal of Biotechnology* **79**, 259-268 (2000).

147 Vroman, L. & Adams, A. Findings with the recording ellipsometer suggesting rapid exchange of specific plasma proteins at liquid/solid interfacs. *Surface Science* **16**, 438-446 (1969).

148 Vogler, E. A. Protein adsorption in three dimensions. *Biomaterials* **33**, 1201-1237, doi:10.1016/j.biomaterials.2011.10.059 (2012).

149 Engel, J. *et al.* SHAPES, DOMAIN ORGANIZATIONS AND FLEXIBILITY OF LAMININ AND FIBRONECTIN, 2 MULTIFUNCTIONAL PROTEINS OF THE EXTRACELLULAR-MATRIX. *J. Mol. Biol.* **150**, 97-120, doi:10.1016/0022-2836(81)90326-0 (1981).

150 Berglin, M. *et al.* Fibrinogen Adsorption and Conformational Change on Model Polymers: Novel Aspects of Mutual Molecular Rearrangement. *Langmuir* **25**, 5602-5608 (2009).

151 Savage, B. & Ruggeri, Z. M. Selective Recognition of Adhesive Sites in Surface-Bound Fibrinogen by Glycoprotein-Iib-Iiia on Nonactivated Platelets. *Journal of Biological Chemistry* **266**, 11227-11233 (1991).

152 Tang, L. P. & Eaton, J. W. Fibrin(Ogen) Mediates Acute Inflammatory Responses to Biomaterials. *Journal of Experimental Medicine* **178**, 2147-2156 (1993).

153 Garcia, A. J., Vega, M. D. & Boettiger, D. Modulation of cell proliferation and differentiation through substrate-dependent changes in fibronectin conformation. *Mol. Biol. Cell* **10**, 785-798 (1999).

154 Keselowsky, B. G., Collard, D. M. & Garcia, A. J. Surface chemistry modulates fibronectin conformation and directs integrin binding and specificity to control cell adhesion. *J. Biomed. Mater. Res. Part A* **66A**, 247-259, doi:10.1002/jbm.a.10537 (2003).

155 Mori, Y. *et al.* A NEW ANTITHROMBOGENIC MATERIAL WITH LONG POLYETHYLENEOXIDE CHAINS. *Transactions American Society for Artificial Internal Organs* **28**, 459-463 (1982).

156 Israelachvili, J. The different faces of poly(ethylene glycol). *Proc. Natl. Acad. Sci. U. S. A.* **94**, 8378-8379, doi:10.1073/pnas.94.16.8378 (1997).

157 Jeon, S. I. & Andrade, J. D. PROTEIN SURFACE INTERACTIONS IN THE PRESENCE OF POLYETHYLENE OXIDE .2. EFFECT OF PROTEIN SIZE. *Journal of Colloid and Interface Science* **142**, 159-166, doi:10.1016/0021-9797(91)90044-9 (1991).

158 Jeon, S. I., Lee, J. H., Andrade, J. D. & Degennes, P. G. PROTEIN SURFACE INTERACTIONS IN THE PRESENCE OF POLYETHYLENE OXIDE .1. SIMPLIFIED THEORY. *Journal of Colloid and Interface Science* **142**, 149-158, doi:10.1016/0021-9797(91)90043-8 (1991).

159 Unsworth, L. D., Sheardown, H. & Brash, J. L. Polyethylene oxide surfaces of variable chain density by chemisorption of PEO-thiol on gold: Adsorption of proteins from plasma studied by radiolabelling and immunoblotting. *Biomaterials* **26**, 5927-5933, doi:10.1016/j.biomaterials.2005.03.010 (2005).

160 Prime, K. L. & Whitesides, G. M. ADSORPTION OF PROTEINS ONTO SURFACES CONTAINING END-ATTACHED OLIGO(ETHYLENE OXIDE) - A MODEL SYSTEM

USING SELF-ASSEMBLED MONOLAYERS. *J. Am. Chem. Soc.* **115**, 10714-10721, doi:10.1021/ja00076a032 (1993).

161 Wang, R. L. C., Kreuzer, H. J. & Grunze, M. Molecular conformation and solvation of oligo(ethylene glycol)-terminated self-assembled monolayers and their resistance to protein adsorption. *Journal of Physical Chemistry B* **101**, 9767-9773, doi:10.1021/jp9716952 (1997).

162 Han, S., Kim, C. & Kwon, D. Thermal/oxidative degradation and stabilization of polyethylene glycol. *Polymer* **38**, 317-323, doi:10.1016/s0032-3861(97)88175-x (1997).

163 Kawai, F. *et al.* BACTERIAL OXIDATION OF POLYETHYLENE-GLYCOL. *Appl. Environ. Microbiol.* **35**, 679-684 (1978).

164 Frazier, R. A. *et al.* Characterization of protein-resistant dextran monolayers. *Biomaterials* **21**, 957-966, doi:10.1016/s0142-9612(99)00270-7 (2000).

165 Capila, I. & Linhardt, R. J. Heparin - Protein interactions. *Angewandte Chemie-International Edition* **41**, 391-412 (2002).

166 Ekblad, T. *Hydrogel Coatings for Biomedical and Biofouling Applications* PhD thesis, Linköping University, (2010).

167 Glasmastar, K., Larsson, C., Hook, F. & Kasemo, B. Protein adsorption on supported phospholipid bilayers. *Journal of Colloid and Interface Science* **246**, 40-47, doi:10.1006/jcis.2001.8060 (2002).

168 Blummel, J. *et al.* Protein repellent properties of covalently attached PEG coatings on nanostructured SiO2-based interfaces. *Biomaterials* **28**, 4739-4747, doi:10.1016/j.biomaterials.2007.07.038 (2007).

169 Kenausis, G. L. *et al.* Poly(L-lysine)-g-poly(ethylene glycol) layers on metal oxide surfaces: Attachment mechanism and effects of polymer architecture on resistance to protein adsorption. *Journal of Physical Chemistry B* **104**, 3298-3309, doi:10.1021/jp993359m (2000).

170 Hansma, H. G. *et al.* Properties of biomolecules measured from atomic force microscope images: A review. *J. Struct. Biol.* **119**, 99-108, doi:10.1006/jsbi.1997.3855 (1997).

171 Höök, F. *Development of a novel QCM-D technique for protein adsorption studies* PhD thesis, Chalmers University of Technology and Göteborg University, (1997).

172 Hook, F. *et al.* Variations in coupled water, viscoelastic properties, and film thickness of a Mefp-1 protein film during adsorption and cross-linking: A quartz crystal microbalance with dissipation monitoring, ellipsometry, and surface plasmon resonance study. *Analytical Chemistry* **73**, 5796-5804 (2001).

173 Malmstrom, J., Agheli, H., Kingshott, P. & Sutherland, D. S. Viscoelastic Modeling of highly hydrated laminin layers at homogeneous and nanostructured surfaces: Quantification of protein layer properties using QCM-D and SPR. *Langmuir* **23**, 9760-9768 (2007).

174 Andersson, O. *Imaging surface plasmon resonance* PhD thesis, Linköping University, (2008).

175 Okamoto, T. & Yamaguchi, I. Optical absorption study of the surface plasmon resonance in gold nanoparticles immobilized onto a gold substrate by self-assembly technique. *Journal of Physical Chemistry B* **107**, 10321-10324, doi:10.1021/jp0345371 (2003).

176 Chah, S., Hutter, E., Roy, D., Fendler, J. H. & Yi, J. The effect of substrate metal on 2-aminoethanethiol and nanoparticle enhanced surface plasmon resonance imaging. *Chemical Physics* **272**, 127-136, doi:10.1016/s0301-0104(01)00423-2 (2001).

177 Lyon, L. A., Pena, D. J. & Natan, M. J. Surface plasmon resonance of Au colloid-modified Au films: Particle size dependence. *Journal of Physical Chemistry B* **103**, 5826-5831, doi:10.1021/jp984739v (1999).